European Journal of Medicinal Chemistry 207 (2020) 112802

Contents lists available at ScienceDirect

European Journal of Medicinal Chemistry

journal homepage: http://www.elsevier.com/locate/ejmech

Research paper

Design, synthesis, antitrypanosomal activity, DNA/RNA binding and *in vitro* ADME profiling of novel imidazoline-substituted 2-arylbenzimidazoles

Andrea Bistrović Popov [a], Luka Krstulović [b], Sanja Koštrun [c, **], Dubravko Jelić [c], Ana Bokulić [c], Marijana Radić Stojković [d], Iva Zonjić [d], Martin C. Taylor [e], John M. Kelly [e], Miroslav Bajić [b], Silvana Raić-Malić [a, *]

[a] Department of Organic Chemistry, Faculty of Chemical Engineering and Technology, University of Zagreb, Marulićev Trg 20, HR-10000, Zagreb, Croatia
[b] Department of Chemistry and Biochemistry, Faculty of Veterinary Medicine, University of Zagreb, Heinzelova 55, HR-10000, Zagreb, Croatia
[c] Fidelta Ltd., Prilaz Baruna Filipovića 29, HR-10000, Zagreb, Croatia
[d] Division of Organic Chemistry and Biochemistry, Laboratory for Biomolecular Interactions and Spectroscopy, Ruđer Bošković Institute, Bijenička 54, HR-10000, Zagreb, Croatia
[e] Department of Infection Biology, London School of Hygiene and Tropical Medicine, Keppel Street, London, WC1E 7HT, UK

ARTICLE INFO

Article history:
Received 26 May 2020
Received in revised form
28 August 2020
Accepted 29 August 2020
Available online 6 September 2020

Keywords:
Imidazoline-substituted benzimidazole
ADME
DNA binding
Trypanosoma brucei

ABSTRACT

Novel imidazoline benzimidazole derivatives containing diversely substituted phenoxy moieties were synthesized with the aim of evaluating their antitrypanosomal activity, DNA/RNA binding affinity and *in vitro* ADME properties. The presence of the diethylaminoethyl subunit in **18a**–**18c** led to enhanced antitrypanosomal potency, particularly for **18a** and **18c**, which contain unsubstituted and methoxy-substituted phenoxy moieties. They were found to be > 2-fold more potent against African trypanosomes than nifurtimox. Fluorescence and CD spectroscopy, thermal denaturation assays and computational analysis indicated a preference of **18a**–**18c** toward AT-rich DNA and their minor groove binding mode. Replacement of the amidine group with less basic and ionisable nitrogen-containing moieties failed to improve membrane permeability of the investigated compounds. Due to structural diversification, the compounds displayed a range of physico-chemical features resulting in variable *in vitro* ADME properties, leaving space for further optimization of the biological profiles.

1. Introduction

Trypanosomatid protozoan parasites have a significant socio-economic impact worldwide [1]. Amongst them are parasites of the *Trypanosoma brucei* species complex, which cause human African trypanosomiasis (HAT), also known as sleeping sickness. In the early stage of the disease, parasites invade the blood and lymphatic system, while in the second stage, they penetrate the blood–brain barrier (BBB) and enter the central nervous system (CNS), leading to coma and death if untreated [2]. The current drugs used to treat HAT, pentamidine, suramin, melarsoprol and nifurtimox-eflornithine combination therapy (NECT), are toxic and not always effective due to the appearance of drug-resistance [1]. In contrast to the treatment of the first-stage HAT that has remained the same for over 60 years, the treatment of second-stage has profoundly evolved. Significant efforts have been made to develop an orally active drug for stage 2 HAT. Nifurtimox, an orally active 5-nitrofuran that readily crosses the BBB and blood-cerebrospinal fluid (CSF) barriers [1] is used in combination with intravenous eflornithine (NECT) to treat gambiense sleeping sickness. Furthermore, the new generation drugs fexinidazole [3–5] and potentially acoziborole [6,7] have been developed for the oral treatment of both stages of HAT. Diamidine drugs such as pentamidine, diminazene and furamidine, are generally ineffective against cerebral trypanosomiasis, although some reports described successes of pentamidine with early-late-stage infections due to its permeability across the BBB by transporters [8,9]. In contrast, pyridyl-substituted analogues of furamidine that are recognized by a BBB

* Corresponding author.;
** Corresponding author.
E-mail addresses: Sanja.Kostrun@fidelta.eu (S. Koštrun), sraic@fkit.hr (S. Raić-Malić).

https://doi.org/10.1016/j.ejmech.2020.112802
0223-5234/

transporter are effective against cerebral trypanosomiasis [10,11]. A limitation of diamidines, which have high therapeutic interest as antiparasitic agents [12], is the requirement for parenteral administration due to poor oral bioavailability resulting from the high pKa of the amidine functional group [13]. Although the active transport of amidines ensures that they reach the site of action, their permanent charge limits membrane permeability and thus oral bioavailability [13,14]. The strategy of incorporating fluorine, chlorine and nitrogen atoms into the aromatic system led to a decrease of the pKa and an increase of antitrypanosomal activity of dicationic bisimidazoline compounds [15]. Although the precise antiprotozoal mechanisms of action have not been fully elucidated, various biological targets have been suggested to account for the activity of aromatic diamidines, including both mitochondrial and nuclear DNA [16], microtubules [17], acidocalcisomes [18], and DNA-targeted enzymes [19]. Compounds that act as kinetoplast DNA (kDNA) binders have been shown to selectively target AT-rich DNA and to form a complex in the minor groove of the double helix that led to destruction of kinetoplast and parasite death [20,21]. It has been found recently that targets for trypanocidal compounds may also include heat shock protein 70 (Hsp70) [22], kinetoplastid proteasome [23] and nuclear receptor PPARγ [24].

Previous studies by our group [25–27] and others [28–36] have shown that nitrogen heterocycles, such as benzimidazole and triazolo-containing derivatives, have good antiprotozoal potency. Herein, we have designed imidazoline benzimidazole derivatives with diversification in the substituted phenoxy moieties, as central part, and right-hand side of a molecule to modulate physico-chemical and biological properties (Fig. 1).

In this study, antitrypanosomal potencies and DNA/RNA binding properties of the compounds were evaluated. Additionally, the binding of newly synthesized compounds with the most promising antitrypanosomal activity to AT-rich DNA was investigated, since selective binding of compounds could be related with their activity. Presumed selectivity toward AT-rich sequences in the minor groove of double-stranded DNA was also investigated by the computational analysis. Furthermore, calculated physico-chemical properties were compared with measured *in vitro* ADME properties, microsomal metabolic stability and membrane permeability.

2. Results and discussion

2.1. Chemistry

The synthesis of novel 2-aryl substituted benzimidazole derivatives **6a**–**6c**, **7a**–**7c**, **8**, **14a**–**18a**, **14b**–**18b** and **14c**–**18c** was carried out as shown in Schemes 1 and 2. Key intermediates for the synthesis of 1,2,3-triazolyl linked 2-aril benzimidazole derivatives (**6a**–**6c**, **7a**–**7c** and **8**) were prepared by regioselective copper(I) catalysed cycloaddition from *O*-propargylated benzaldehydes (**2a**–**2c**), used as dipolarophiles, and corresponding azides (Scheme 1).

1-Benzyl-1,2,3-triazole benzaldehydes **3a**–**3c** were synthesized in excellent yield (82–92%) in a *one-pot click* reaction, 1,3-dipole was formed *in situ* using Cu(II) acetate as a catalyst. 1,3-Dipolar cycloaddition of terminal alkynes (**2a**–**2c**) and 2-(4-morpholine) ethyl azide yielded the corresponding 1-ethylmorpholine-1,2,3-triazole benzaldehyde precursors **4a**–**4c**. The ethylmorpholine substituent was introduced to the N-1 position of the 1,2,3-triazole ring to increase the solubility of imidazoline-substituted benzimidazole derivatives **7a**–**7c**. To determine the influence of substituents on the triazole ring on pharmacokinetic properties and trypanosomal activity, non-substituted triazole **5** was prepared with copper(I) iodide and trimethylsilylazide ($TMSN_3$). Condensation of 4-(1,2,3-triazol-1-yl)benzaldehyde derivatives **3b**, **3c**, **4a**–**4c** and **5** with 4-(imidazolin-2-yl)benzene-1,2-diamine and $NaHSO_3$ or *p*-benzoquinone, as an oxidative reagent, afforded the target imidazoline-substituted benzimidazoles (**6b**–**6c**, **7a**–**7c** and **8**). The 4-(imidazolin-2-yl)benzene-1,2-diamine was prepared by the Pinner reaction previously reported in literature [37]. Furthermore, to look into the influence of the imidazoline substituent, unsubstituted benzimidazole derivative **6a** was prepared by cyclization of *o*-phenylene diamine with benzaldehyde **3a** in 94% yield. With the aim of assessing the influence of the triazole moiety on the antitrypanosomal activity and pharmacokinetic properties, morpholinoyl (**14a**–**14c**), benzoyl (**15a**–**15c**), pyridine (**16a**–**16c**), ethylmorpholine (**17a**–**17c**) and diethylaminoethyl (**18a**–**18c**) substituents were introduced to the phenoxymethylene linker of the imidazoline-substituted benzimidazoles as displayed in

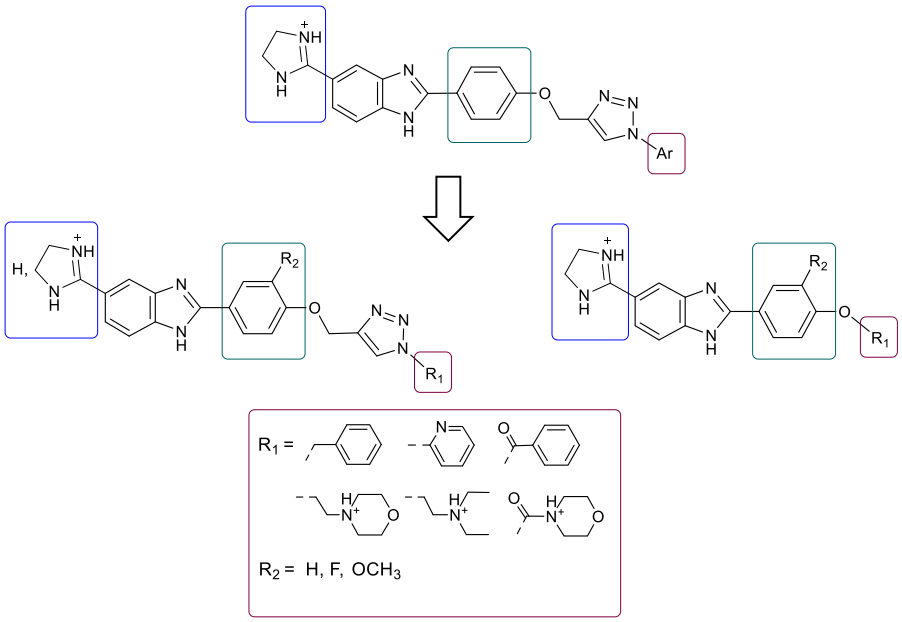

Fig. 1. Design of novel imidazoline-substituted benzimidazoles **6a**–**6c**, **7a**–**7c**, **8**, **14a**–**18a**, **14b**–**18b** and **14c**–**18c** with a range of cyclic, aromatic as well as ionisable aromatic and aliphatic subunits.

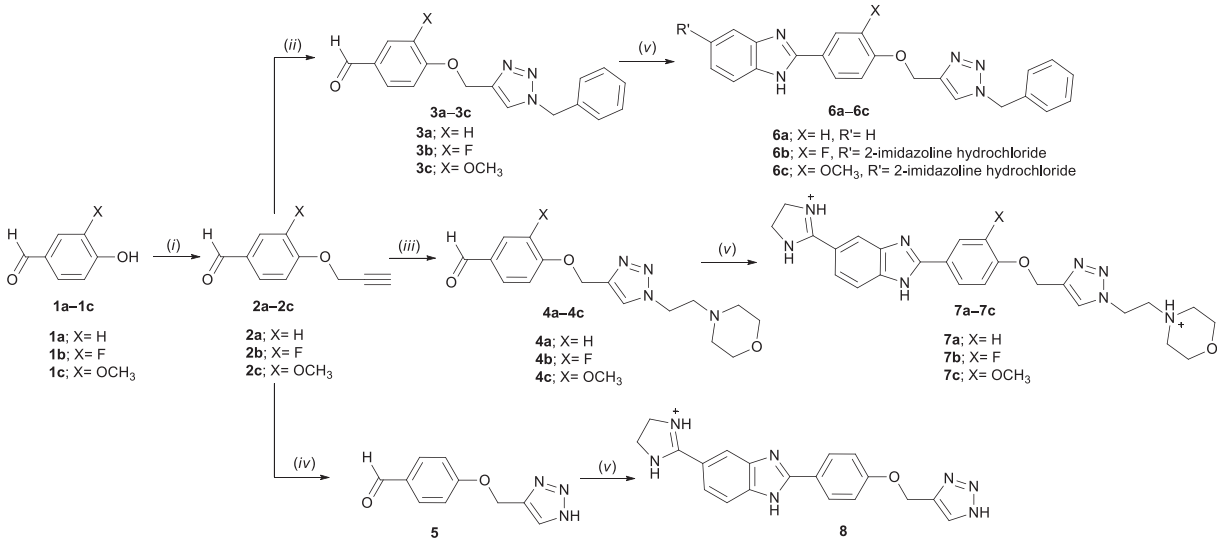

Scheme 1. *Reagents and conditions*: (*i*) propargyl bromide, CH_3CN, K_2CO_3, reflux 8 h; (*ii*) benzyl chloride, NaN_3, Et_3N, 30 min, rt, $Cu(OAc)_2$, *t*-BuOH: H_2O = 1 : 1, 24 h; (*iii*) 4-(2-azidoethyl)morpholine, $Cu(OAc)_2$, MeOH, reflux, 24 h; (*iv*) CuI, $TMSN_3$, DMF: H_2O = 9 : 1, reflux, 6 h; (*v*) 4-(imidazolin-2-yl)benzene-1,2-diamine/1,2-phenylendiamine, $NaHSO_3$/*p*-benzoquinone, EtOH, reflux, 8 h.

Scheme 2. O-alkylation of the hydroxybenzaldehydes **1a**–**1c** with the corresponding halides and K_2CO_3 afforded the benzaldehyde precursors **9a**–**13a**, **9b**–**13b** and **9c**–**13c**, which were converted to target 2-aryl-5-(2-imidazolinyl)-substituted benzimidazole (**14a**–**18a**, **14b**–**18b** and **14c**–**18c**) hybrids with $NaHSO_3$ or *p*-benzoquinone.

2.2. Antitrypanosomal evaluations

Preliminary screening of 2-aryl-substituted benzimidazole derivatives **6a**–**6c**, **7a**–**7c**, **8**, **14a**–**18a**, **14b**–**18b** and **14c**–**18c** against *T. brucei* was performed at different concentrations (100, 10, 1 and 0.1 μg/mL) using the resazurin assay to monitor growth (Materials and methods) (Table S1). All compounds displayed 100% growth inhibition at the highest concentration of 100 μg/mL, while at 10 μg/mL, the aromatic phenoxymethylene pyridine **16b** had the lowest inhibition (40%). Best selectivity was observed with **6a**, **7a**, **8** and **18a**–**18c**, which inhibited growth by more than 90% at 1 μg/mL. Therefore, these compounds were selected for further antitypanosomal activity evaluations and their IC_{50} and IC_{90} values were determined (Table 1).

Cytotoxicity was assessed using the rat myoblast cell line L6. In terms of trypanosoma growth inhibition, imidazoline benzimidazoles **7a**, **7b** and **8**, with the phenoxymethylene-1,2,3-triazole unit, exhibited the lowest activity of the compounds re-tested. Previously, comparing **7a** and **7b** to the corresponding analogues **17a** and **17b**, in which the ethylmorpholine is directly attached to phenoxy core, we had demonstrated that the 1,2,3-triazole linker does improve activity (Table 1, Fig. 2). The 2-arylbenzimidazole **6a**, which lacks the cationic imidazoline moiety, showed activity (IC_{50} = 3.75 μM) comparable to that of nifurtimox. However, this compound was also relatively cytotoxic (IC_{50} = 17.2 μM) with a selectivity index (S.I.) of 4.6. Introduction of the diethylaminoethyl substituent attached to phenoxymethylene in **18a**–**18c** led to considerably increased and selective activity, particularly **18a** and **18c** that exhibited IC_{50} values in sub-micromolar range (**18a**: IC_{50} = 0.47 μM, IC_{90} = 1.82 μM; **18c**: IC_{50} = 0.73 μM, IC_{90} = 1.47 μM). These compounds were non-cytotoxic (S.I. > 530). Interestingly, addition of the electron-withdrawing fluorine into **18b** resulted in a 6-fold reduction in antitrypanosomal activity compared to non-

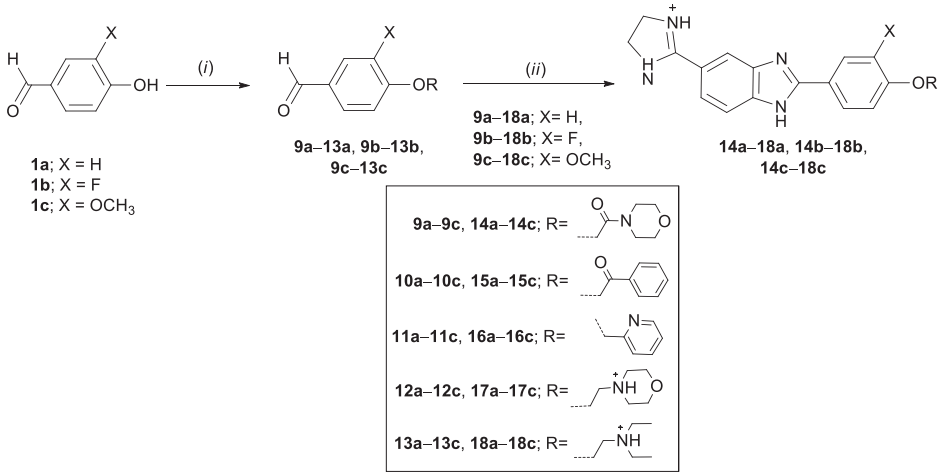

Scheme 2. *Reagents and conditions*: (*i*) RCl/RBr, CH_3CN, K_2CO_3, reflux, 8 h; (*ii*) 4-(imidazolin-2-yl)benzene-1,2-diamine, $NaHSO_3$/*p*-benzoquinone, EtOH, reflux, 8 h.

Table 1
Antitrypanosomal activity[a] of compounds **6a**, **7a**, **7b**, **8**, and **18a**–**18c** against cultured bloodstream form *T. b. brucei* (Materials and methods).

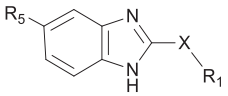

Cmpd	X	R1	R5	*T. brucei*		L6 cells	S.I.[c]
				IC_{50} (μM)	IC_{90} (μM)	IC_{50} (μM)	IC_{50} (Tb/L6)
6a	-$PhOCH_2$-	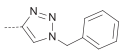	H	3.75 ± 0.06	-	17.2 ± 0.8	4.6
7a	-$PhOCH_2$-	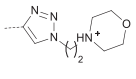		>4	-	-	-
7b	-$FPhOCH_2$-	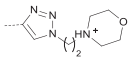		>4	-	-	-
8	-$PhOCH_2$-			>4	-	-	-
18a	-$PhOCH_2$-			0.47 ± 0.02	1.82 ± 0.15	>250	>530
18b	-$FPhOCH_2$-			3.67 ± 0.30	-	>250	>68
18c	-$CH_3OPhOCH_2$-			0.71 ± 0.22	1.47 ± 0.22	>250	>350
Nifurtimox[b]	-	-		2.0 ± 0.2[b]	-		

[a] *In vitro* activity against bloodstream form *T. brucei* expressed as the concentration that inhibited growth by 50% (IC_{50}) and 90% (IC_{90}). Data are the mean of triplicate experiments ± SEM.
[b] Taken from Ref. [38].
[c] Selectivity index; SI = [IC_{50} L6 cells]/[IC_{50} *T. brucei*].

substituted structural congener **18a**, whereas analogue **18c**, with an electron-donating methoxy group showed comparable activity to **18a**.

2.3. DNA and RNA binding study

Based upon antitrypanosomal activity, compounds **18a**–**18c** were selected for the binding study with DNA and RNA. As previously mentioned, dicationic molecules with antitrypanosomal activity, such as the bis(2-aminoimidazoline) drugs, were found to be DNA minor groove binders, with selectivity toward AT-sequences [21,39]. The research on aromatic diamidines demonstrated a correlation between the structure, antitrypanosomal activity and their ability to bind to the AT-sequences in the minor groove [21,40]. Thus, the aim of this study was to further examine DNA and RNA interactions with highly active trypanocides **18a**–**18c**. The binding study with ds-RNA aimed to prove the preferable binding of compounds to AT-DNA (recognition of polynucleotide conformation and/or bases) in comparison to GC-DNA and RNA. The UV/Vis spectra (Figs. S1–S5, Supporting Information, SI) of buffered

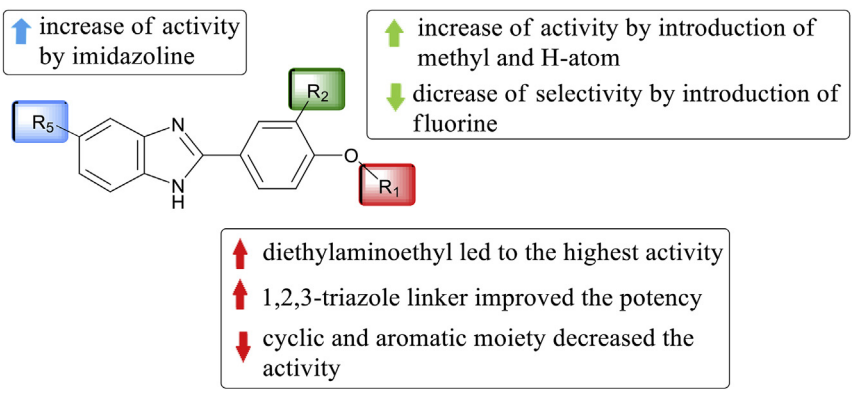

Fig. 2. Structure–activity relationship for antitrypanosomal activity of the imidazoline-substituted 2-arylbenzimidazoles.

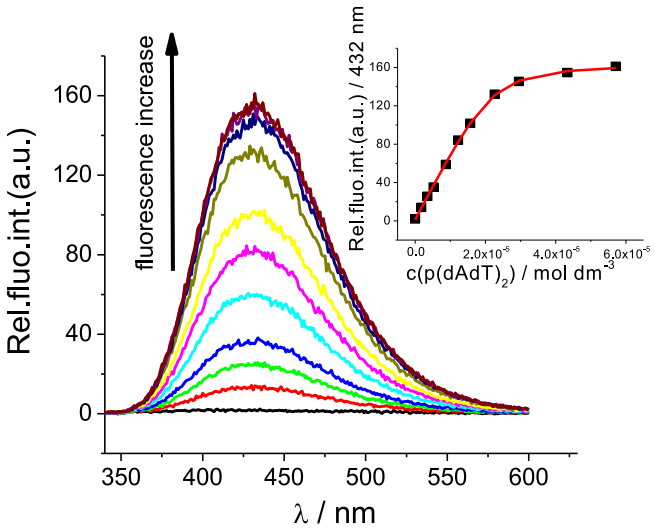

Fig. 3. Changes in fluorescence spectrum of **18c** ($c = 1 \times 10^{-6}$ mol dm^{-3}, $\lambda_{exc} = 320$ nm) upon titration with poly(dAdT)$_2$ ($c = 1.7 \times 10^{-6} - 5.7 \times 10^{-5}$ mol dm^{-3}); Inset: dependence of **18c** absorbance at $\lambda = 432$ nm on c(poly(dAdT)$_2$), at pH = 7, sodium cacodylate buffer, $I = 0.05$ mol dm^{-3}.

solutions of **18a**–**18c** were proportional to their concentrations up to $c = 2 \times 10^{-5}$ mol dm^{-3}, suggesting that these compounds do not aggregate by intermolecular stacking at the experimental conditions used. The absorption maxima and the corresponding molar extinction coefficients (ε) are given in Table S2 (SI). Changes in the UV/Vis spectra of the compounds as the temperature increased to 95 °C were negligible, and the reproducibility of UV/Vis spectra upon cooling back to 25 °C was excellent. The excitation spectra agreed well with the corresponding absorption spectra in the region where emission and excitation spectrum do not overlap (Figures S6-S13, SI). Binding of the compounds to DNA and RNA polynucleotides was monitored by fluorescence spectroscopy. CD titrations and ΔT_m experiments were used to determine the binding modes (intercalation, groove binding or external binding). To assess the binding selectivity and sequence-specific recognition of evaluated compounds, for initial measurements with ds-polynucleotides, we chose *calf thymus* DNA (ctDNA), which represents a classical B-helix, and poly A – poly U, as a model for RNA, with a characteristic A-helical structure of a wide and shallow minor groove and a deep and narrow major groove [41]. After acquiring preliminary results with ctDNA, we decided to perform experiments with synthetic polynucleotides, poly(dAdT)$_2$ and poly(dGdC)$_2$, both of which form a classical B-helix, but in the case of the latter, with a minor groove that is sterically hindered by the amino groups of guanine [42]. Polynucleotide addition to compound solutions resulted in an emission increase of **18c**, and fluorescence quenching of **18a** and **18b** (Fig. 3, Table 2).

18a and **18b** showed dual fluorimetric responses in titrations with AT-DNA (poly(dAdT)$_2$). First additions of this polynucleotide induced a decrease in **18a** and ***18b*** fluorescence, while further aliquots yielded a significant fluorescence increase. Unlike **18a** and **18b**, the emission maximum of **18c** did not shift on its binding to most of the studied polynucleotides. Fluorescence changes of **18c** with GC-DNA were too small for accurate calculation of binding constants (Table 2).

Interestingly, **18a**–**18c**, that differ only in the phenyl substitution (H vs F vs OCH_3), caused opposite fluorimetric changes on interaction with the studied polynucleotides. While the addition of **18a** and **18b** caused a decrease in fluorescence in the presence of DNA/RNA, the addition of any polynucleotides resulted exclusively in a strong emission increase of **18c**, which may be ascribed to an increased electron density in the phenyl ring due to the electron-donating methoxy group (Figures S14-S25, SI).

The binding constants *Ks* and ratios $n_{[bound\ compound]/[DNA/RNA]}$ obtained by processing of fluorimetric titration data with the Scatchard equation [43] are summarized in Table 3. All compounds showed greater affinity toward DNA, especially AT-DNA. In particular, **18c** exhibited AT-DNA selectivity over GC-DNA.

Non-covalent binding of small molecules to ds-polynucleotides usually has certain effects on the thermal stability of helices, thus, giving different melting temperature (T_m) values. Melting temperature depends on both the length and the specific nucleotide sequence composition of the polynucleotide. It can be also influenced by salt concentration and pH. Differences between the T_m value of the free polynucleotide and that obtained in complex with small molecules (ΔT_m value) is an important factor in the characterisation of small molecule-ds-polynucleotide interactions [44]. All studied compounds showed a smaller stabilization effect of ds-RNA (poly A – poly U) compared to ds-DNA (Table 3).

Furthermore, all compounds showed a significant but smaller stabilization effect toward mixed DNA base pairs than to AT-DNA. This difference in stabilization effect can be explained by ctDNA composition which contains 58% AT and 42% GC nucleobases [45].

Compounds **18a**, without a substituent on the phenyl, and **18c**, with a methoxy-substituted phenyl moiety, showed the best stabilization effect of AT-DNA (Table 3). Such AT preference is characteristic of small molecules that bind into a minor groove of ds-polynucleotides [16,45]. In the case of ds-RNA, the minor grove is not the probable binding site with these compounds, since it is broad and shallow, in contrast to the deep and narrow minor groove of the ds-DNA [42].

To get insight into conformational changes in the secondary

Table 2
Binding constants (log*Ks*)[a] and ratios *n*[b] ([bound compound]/[polynucleotide phosphate]) calculated from the fluorescence titrations of **18a**–**18c** with ds-polynucleotides at pH = 7.0 (buffer sodium cacodylate, $I = 0.05$ mol dm^{-3}).

	ctDNA			poly A – poly U			p(dAdT)$_2$			p(dGdC)$_2$		
	logK_s	*n*	I/I$_0$[d]	logK_s	*n*	I/I$_0$[d]	logK_s	*N*	I/I$_0$[d]	logK_s	*n*	I/I$_0$[d]
18a	5.9	0.2	0.5	5.1	0.2	0.4	5.2	0.1[c]	2.0	5.3	<0.1	<0.1
18b	6.0	0.1	0.3	4.9	0.2	0.2	6.4	0.1[c]	1.3	4.5	0.4	<0.1
18c	6.8	<0.1	43.4	5.4	<0.1	23.7	7.1	<0.1	146	-[e]	-[e]	-[e]

[a] Accuracy of $n \pm 10$–30%, consequently log*Ks* values vary in the same order of magnitude.
[b] Processing of titration data using Scatchard equation [43] gave values of ratio *n*[bound compound]/[polynucleotide]; correlation coefficients were >0.99 for most of calculated K_a.
[c] In case of **18a** and **18c** with poly(dAdT)$_2$, logK_a values (part of titration experiment where emission increased) were re-calculated for fixed $n = 0.1$ due to a more reliable fit than with free stoichiometry; logK_a values could not be calculated from part of titration where **18a** and **18c** emission decreased since these changes were too small for accurate calculation of binding constants.
[d] I_0 – starting fluorescence intensity of **18a**–**18c**; I – fluorescence intensity of **18a**–**18c**/polynucleotide complex calculated by Scatchard equation.
[e] Fluorescence changes of studied compound with polynucleotides were too small for accurate calculation of binding constants.

Table 3
The ΔT_m[a] values (°C) of ds-polynucleotides upon addition of ratio ***r***[b] = 0.3 of **18a**–**18c** at pH = 7.0 (sodium cacodylate buffer, I = 0.05 mol dm^{-3}).

	ctDNA	poly A − poly U	poly (dA − dT)$_2$
18a	6.4	4.5	17.9
18b	4.5	2.4	14.7
18c	7.2	2.3	19.3

[a] Error in ΔT_m: ± 0.5 °C.
[b] ***r*** = [compound]/[polynucleotide].

structure of polynucleotides upon small molecule binding, CD spectroscopy was employed [46]. Additional information on the ligand-polynucleotide complexes can be acquired *via* an induced CD (ICD) signal of achiral small molecules when they form complexes with ds-polynucleotides. From this, a mutual orientation of the small molecule and polynucleotide chiral axis can be derived, giving useful information on the modes of interaction [47,48]. The ICD signals observed at λ > 300 nm can be attributed solely to the studied achiral compounds, since they display UV/Vis spectra in this region while polynucleotides do not (Fig. 4, Figures S1-S4, SI).

Addition of the compounds resulted in a decreased intensity of the CD band of RNA and DNA polynucleotides (Figures S29-S30, SI). Conversely, increased intensity of CD band of poly(dGdC)$_2$ was noticed on addition of all the studied compounds. All compounds exhibited positive induced CD spectra (ICD) with ctDNA and poly(dAdT)$_2$ in the region from 330 to 340 nm (Fig. 4, Figures S29 and S30, SI). Such changes were observed for cationic benzimidazoles and indoles that were found to be minor groove binders [16,48]. The positive ICD spectra, located around 336 nm, were also observed in titrations of poly A − poly U with all compounds studied (Figs. S29 and SI). Additionally, clear isodichroic points were observed in titrations of **18a** with AT-DNA and **18c** with poly A − poly U, suggesting one dominant interaction mode of these compounds with the DNA/RNA chiral axis [47,48].

A positive ICD band, with an intensity similar or stronger than the CD band of DNA/RNA, strongly supports the minor groove binding to DNA, or the major groove binding to ds-RNA [49]. Thus, it can be concluded that the compounds bind to the minor groove of ds-DNA and to major groove of ds-RNA. Preferable binding to the minor groove of AT-DNA is additionally supported by strong

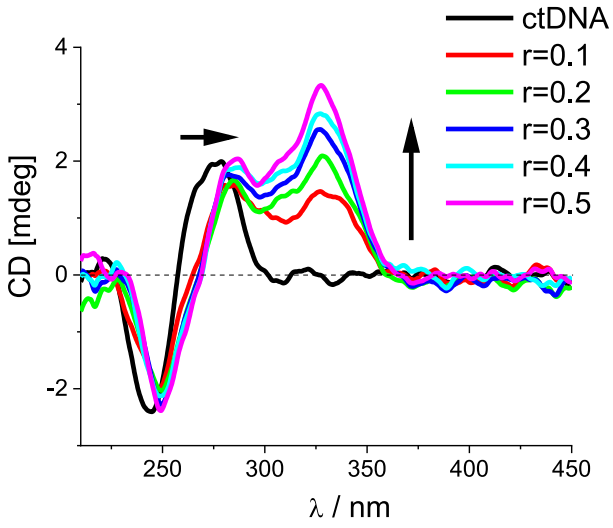

Fig. 4. CD titration of ctDNA (c = 3.0 × 10^{-5} mol dm^{-3}) with **18a** at molar ratios ***r*** = [compound]/[polynucleotide] (pH = 7.0, buffer sodium cacodylate, I = 0.05 mol dm^{-3}).

stabilization effects (Table 3) and high binding affinities (1–10 μM, Table 2). The appearance of a dual fluorimetric response in the titrations of **18a** and **18b** with AT-DNA, suggests two different modes of binding, probably monomer binding inside the groove at ratios ***r*** [**18a**, **18b**]/[poly(dAdT)$_2$] < 0.2 and formation of lower-order aggregates of **18a** and **18 b** at ratios ***r*** > 0.2. The intensity of the CD spectrum of poly(dGdC)$_2$ significantly increased upon addition of all compounds and there were no ICD bands at wavelengths longer than 300 nm. Such changes suggest a non-intercalative mode of binding, probably aggregation along the polynucleotide backbone, most likely inside the hydrophobic major grooves [50].

2.4. Computational analysis of imidazoline-substituted benzimidazoles binding to DNA

To further investigate and rationalize results obtained by fluorescence and CD spectroscopy, binding of **18a**–**18c** to the DNA minor groove at the molecular level were investigated by computational methods. Their selectivity towards the AT sequences was investigated as well.

Available X-ray structures of DNA complexes with binders, structurally related to imidazoline-substituted benzimidazoles, were retrieved from the Protein Databank [51–53] and all DNA-ligand complexes and interactions were analysed (pdb codes: 1D30, 1D64, 1DNH, 109D, 1FTD, 1M6F, 1Z8V, 1JTL, 1RMX, 2DND, 2B0K, 2GYX, 442D, 445D, 403D, 458D/459D, 4AH1, 432D, 5T4W, 5LIT, 6BNA, 6EL8). However, for further computational experiments following X-ray structures were used as representatives of the AT-rich DNA complexes: crystal structure of the DB921-D(CGCGAATTCGCG)2 complex (pdb: 2B0K) and the structure of the DNA duplex d(AAATTT)2 with the potential antiparasitic drug 6XV (pdb: 5LIT). Crystal structure of the Forkhead domain of human FOXN1 in complex with human ctDNA (6EL8) was used for selectivity investigation. Structures of inhibitors and their interactions with DNA are given in Fig. 5a and b. DB921-D(CGCGAATTCGCG)2 complex (pdb: 2B0K) is an example of water mediated interaction between inhibitor and DNA, compensating for the lack of iso-helical structure, while 6XV-d(AAATTT)2 complex (pdb: 5LIT) is an example of direct binding with three well oriented H-bonds.

Compounds **18a**–**18c** were docked to the X-ray templates of DNA as described in the Methods section. Both, water mediated and direct binding to the minor groove of the DNA were examined as shown for compound **18c** in Fig. 5c and d. Complexes were further optimised by the MMGBSA method, and the energy of interaction for compound **18c** is shown in Table 4 in comparison with 2B0K ligand.

Compounds **18a**–**18c** could bind directly as well as through water mediated interactions to compensate the deviations from isohelical structures as shown in Fig. 5 for compound **18c**. Both complexes form three hydrogen bonds with the DNA bases, with the only difference noticed being for the interaction of the diethylamino group. In the case of water mediated binding, all hydrogen bonds are formed with chain A of the DNA helix, while in the direct complex, the diethylamino group forms a hydrogen bond with the C21 of the chain B. At 2.5 Å, this is slightly longer than the other two strong H-bonds of 1.8 and 2.0 Å, respectively.

For the most active compounds shown in the Table 1, deviation from the ideal isohelical structure is around 20°, comparable to a DAPI molecule (pdb: 1D30), and the deviation from the linear geometry is around 30°.

As already shown for a number of minor groove binders [13,53–55], lack of an isohelical structure could be efficiently compensated for by water mediated interactions. In order to investigate which complex would be energetically favourable,

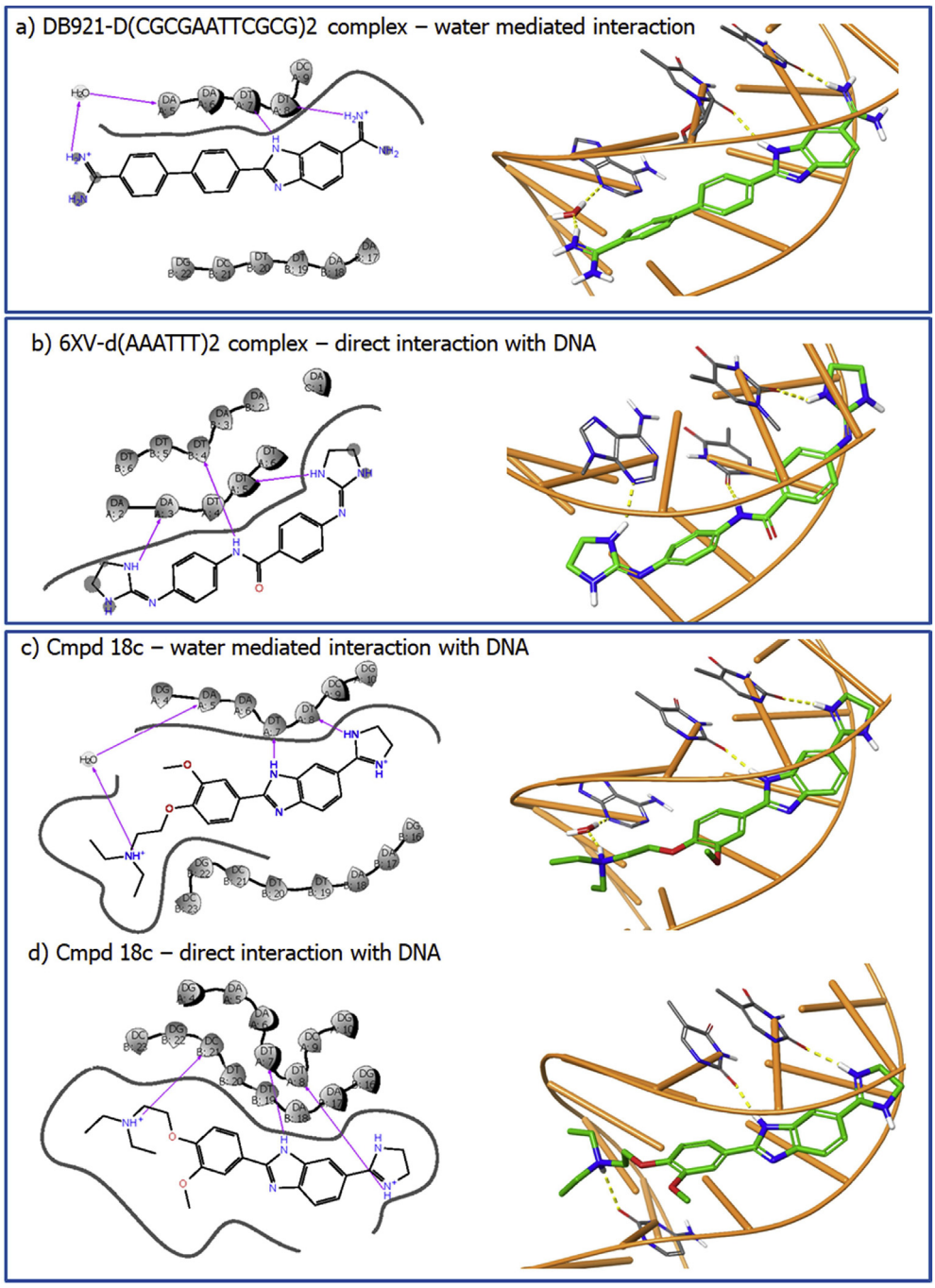

Fig. 5. DNA interactions with a) DB921 (pdb: 2B0K), b) 6XV (pdb: 5LIT), c) and d) compound **18c** docked into pdb: 2B0K.

docked geometries were re-optimised and free energies of interaction were calculated by the MMGBSA method. We employed molecular mechanics to estimate the strength of interaction and a generalised Born model and solvent accessibility method to implicitly describe solvent effects. Results are shown in Table 4 for the 2B0K ligand, as reference, and compound **18c**. It can be seen, from the calculated free energies, that the 2B0K ligand forms a more stable water mediated complex, while for compound **18c**, direct interactions are more favourable. This is not surprising since the flexible diethylaminoethyl chain can easily adopt a conformation that enables the formation of H-bonds with DNA bases. In addition, molecular dynamic simulations were performed to check the dynamics of ligand-DNA interactions. In the case of 2B0K, two direct and one water mediated hydrogen bond is formed and maintained throughout the whole simulation time. For the **18c**

Table 4
Ligand ΔG(int)/kcalmol^{-1} with AT-rich DNA (pdb: 2B0K) and ctDNA (pdb: 6EL8).

Cmpd	AT-rich DNA	AT-rich DNA + water	ctDNA	ctDNA + water
2B0K ligand	−80	−84	−68	−73
18c	−100	−75	−84	not forming

Table 5
Measured metabolic stability in mouse liver microsomes (Pred *in vivo* hep CL) and apparent permeability (P_{app}) in MDCKII-hMDR1 cell assay from apical-to-basolateral (AB) and basolateral-to-apical (BA) side and calculated physico-chemical and structural properties.

Cmpd	Measured properties				Calculated properties									
	Pred *in vivo* hep CL [% LBF]	P_{app} (AB) [$\times 10^{-6}$ cm/s]	P_{app} (BA) [$\times 10^{-6}$ cm/s]	Efflux ratio	TPSA[a]	AR[b]	RB[c]	HBD[d]	HBA[e]	LogP	LogD	Solubility in water	pKa	PPB[f] (%)
6a	74.22	12.49	N/A	N/A	68.6	5	6	1	6	4.15	4.15	Highly insoluble	5.2	99.62
6b	84.37	<0.1	0.09	N/A	93.0	5	7	2	8	3.07	1.21	Insoluble	12.6	98.92
6c	79.00	<0.1	<0.1	N/A	102.2	5	8	2	9	2.67	0.81	Insoluble	10.9	98.98
7a	47.87	1.09	1.18	1.09	105.5	4	8	2	10	1.2	−0.7	Soluble	10.9/7.4	88.65
7b	73.42	0.49	0.80	1.64	105.5	4	8	2	10	1.32	−0.58	Soluble	12.6/7.4	89.15
7c	64.14	0.48	0.89	1.86	114.7	4	9	2	11	1.17	−0.73	Very soluble	10.9	89.55
8	<30	0.46	0.84	1.81	103.9	4	5	3	8	1.58	−0.26	Slightly soluble	11.0	91.08
14a	<30	1.06	1.53	1.44	91.8	3	5	2	8	1.14	−0.72	Slightly soluble	10.9	92.85
14b	34.32	0.86	0.99	1.16	91.8	3	5	2	8	1.27	−0.59	Insoluble	12.6	93.58
14c	<30	1.76	1.38	0.78	101.1	3	6	2	9	0.98	−0.88	Slightly soluble	10.9	88.31
15a	87.06	<0.1	0.11	N/A	79.4	4	6	2	6	3.09	1.23	Insoluble	10.9	99.2
15b	92.59	<0.1	<0.1	N/A	79.4	4	6	2	6	3.17	1.31	Insoluble	12.6	98.15
15c	90.38	<0.1	N/A	N/A	88.6	4	7	2	7	3.08	1.22	Insoluble	10.9	98.63
16a	<30	0.07	0.51	7.82	75.2	4	5	2	6	2.62	0.76	Insoluble	12.7	97.68
16b	<30	<0.1	0.2	>2.4	75.2	4	5	2	6	2.7	0.84	Insoluble	12.6	96.71
16c	<30	0.12	0.52	4.22	84.4	4	6	2	7	2.24	0.38	Insoluble	12.7	96.81
17a	66.97	0.49	0.69	1.40	74.8	3	6	2	7	1.81	−0.09	Soluble	12.7/7.1	82.86
17b	65.49	0.49	0.84	1.70	74.8	3	6	2	7	1.86	−0.03	Soluble	12.5/7.0	86.93
17c	47.79	0.64	0.67	1.04	84.0	3	7	2	8	1.66	−0.25	Soluble	12.7/7.0	82.8
18a	<30	0.27	0.63	2.38	65.5	3	8	2	6	2.99	−0.71	Soluble	12.5/8.9	90.82
18b	<30	0.17	0.49	2.92	65.5	3	8	2	6	2.87	−0.88	Soluble	12.7	89.63
18c	<30	<0.1	0.50	>5.0	74.8	3	9	2	7	2.57	−1.20	Slightly soluble	12.7/9.0	89.41

[a] Total polar surface area.
[b] Number of aromatic rings.
[c] Number of rotatable bonds.
[d] Number of hydrogen bond donors.
[e] Number of hydrogen bond acceptors.
[f] Plasma protein binding.

ligand, in addition to two direct H-bonds, a third H-bond is formed both directly and bridged by a water molecule, increasing the probability of strong interaction.

Findings from these structural studies are in agreement with the observed antitrypanosomal activity, since the most active compounds, **18a**–**18c**, possess a flexible and also most basic diethylaminoethyl group. However, compounds with more rigid, 3D shaped and less basic morpholine, pyridine and phenyl moieties exhibit lower activity and were predicted to bind weaker to the DNA. ΔG(int) values of compounds **16c** and **17c** are −85 and −94 kcal mol^{-1} for the AT-rich DNA.

Furthermore, compound **18c** binds with higher selectivity to AT-rich DNA in comparison to ctDNA, as shown by calculated free binding energies (Table 4).

To further explore the dynamics of water mediated ligand-DNA interactions, molecular dynamic simulations in water as a solvent were performed for 20 ns at room temperature to ensure stability of the DNA oligomers [56]. Simulations were carried out for 2B0K and **18c** ligands. MMGBSA optimised complex structures were used as starting points. The average number of direct H-bonds during the simulation is in agreement with docking and MMGBSA predictions, while water mediated H-bonds are more dynamic and occur with lower frequency than direct H-bonds, as shown in Fig. 6.

2.5. In vitro ADME profiling

Metabolic stability in mouse liver microsomes and permeability in the MDCKII-hMDR1 assay were determined for synthesized imidazoline-substituted benzimidazole derivatives and the results are shown in Table 5. In addition, lipophilicity, solubility, potential for CYP inhibition and metabolism, binding to plasma proteins and structural parameters were calculated by ACD Percepta software (Table 5). Metabolic studies have shown that majority of compounds have low (<30% liver blood flow, LBF) to moderate clearance (30–70% LBF), while compounds **6a**–**6c** and **15a**–**15c** with phenyl ring have high clearance (>70% LBF), indicating the impact of the substituent at the triazole and phenoxy unit on metabolic stability. Thus, in the series of compounds with the triazole moiety, imidazoline benzimidazole **8** with an unsubstituted triazole, showed low clearance and high stability in microsomes, whereas ethylmorpholine-substituted analogues **7a**–**7c** and, particularly, the benzyl-substituted derivatives **6a**–**6c**, exhibited reduced microsomal stability. Among the series containing a phenoxy core directly substituted with cyclic, aromatic and aliphatic moieties, morpholinoyl (**14a**–**14c**), methylpyridine (**16a**–**16c**) and diethylaminoethyl (**18a**–**18c**) substitution improved the metabolic stability.

Although compounds were designed to contain one, instead of two amidine moieties, they were all characterized by low membrane permeability ($P_{app}(AB) < 2 \times 10^{-6}$ cm/s). High efflux was also measured for compounds **16a**, **16c** and **18a**–**18c**. A major bottleneck to the membrane permeability is the permanently charged amidine moiety. Compound **6a**, which does not contain an amidine group, has a high AB permeability of 12.49×10^{-6} cm/s. However, the amidine moiety was shown to be important for the DNA binding and active transport into the parasitic cell, as evidenced by the

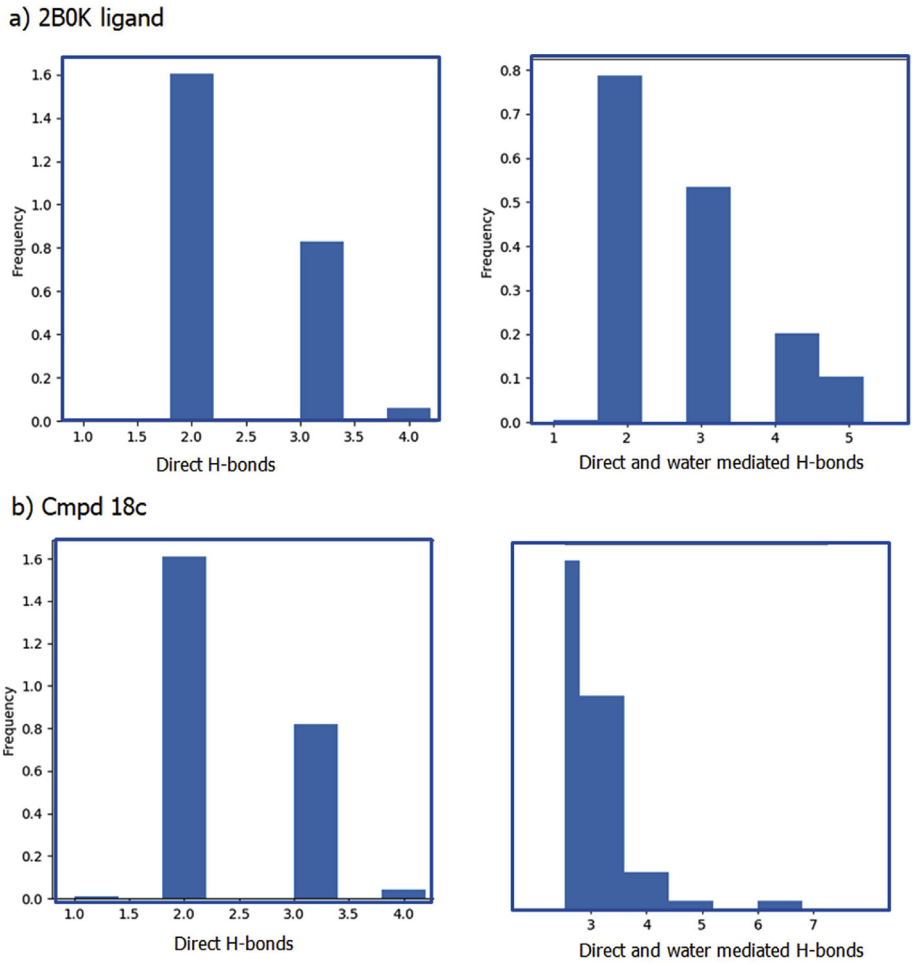

Fig. 6. Average number of direct H-bonds (left-hand side) and average number of hydrogen bonds as a sum of direct and water-mediated interactions (right-hand side) during MD simulation for a) 2B0K and b) **18c** ligands.

observed antitrypanosomal activity of bisamidines [13,21]. Therefore, modulation of amidine basicity will be essential in order to increase membrane permeability and to retain biological activity. pKa values were predicted to range from 11 to 13 for amidine moieties, around 9 for aliphatic amines, and around 7 for morpholine derivatives, which is in agreement with the published data [57–59]. Imidazoline benzimidazoles fall in the good lipophilicity range, with a calculated logP spanning from 1.14 to 3.17, and logD from −1.2 to 1.31. Non-amidino benzimidazole **6a** has logP value of 4.15. Binding to plasma proteins (PBP) is predicted to be lower than 91% for imidazoline benzimidazoles, with ethylmorpholine (**7a**–**7c** and **17a**–**17c**) and diethylaminoethyl (**18a**–**18c**), ensuring an acceptable drug free fraction, while compounds **6a**–**6c** with N-1 benzyl-substituted triazole showed the highest binding (>99% PBP).

Compounds containing ionisable groups (**7a**–**7c**, **17a**–**17c** and **18a**–**18c**) are predicted to have good water solubility. Overall, the physico-chemical and *in vitro* ADME properties could be favourably modulated within the current chemical series, with exception of a consistently low membrane permeability.

3. Conclusions

The imidazoline-substituted benzimidazoles with a range of cyclic, aromatic and ionisable aromatic and aliphatic substituents to a phenoxy central core were synthesized and evaluated for their antitrypanosomal activity. Generally, the type of substituents had profound effects on antiprotozoal activities. While a triazole spacer between the phenoxymethylene and the ethylmorpholine (in **7a** and **7b**), and the benzyl moiety (in **6a**), led to improved and rather unselective activity, the diethylaminoethyl directly attached to phenoxy in **18a**–**18c** significantly increased the potency with IC_{50} values in the range of 0.47–3.67 μM. Furthermore, introduction of an electron-withdrawing fluorine (**18b**) resulted in decreased growth inhibition, while non-substituted and electron-donating methoxy-substituted phenoxy moieties (**18a** and **18c**) showed comparable antitrypanosomal activity.

Fluorescence and CD spectroscopy, as well as the thermal denaturation assay showed large stabilization effects of AT-DNA, high binding affinities (1–10 μM) with both ctDNA and AT-DNA and large positive ICD spectra for **18a**–**18c** that point to their preference toward AT-rich DNA sequences and minor groove binding mode. These results were supported by computational analysis, which showed that compounds **18a**–**18c** with a conformationally unrestricted diethylaminoethyl chain, in comparison to the rigid analogues with cyclic and aromatic moieties, have stronger interaction to DNA and can bind with higher selectivity to AT-rich DNA, in comparison to ctDNA.

In vitro ADME profiling showed that the imidazoline-substituted benzimidazoles with ionisable ethylmorpholine (**7a**–**7c** and **17a**–**17c**) and diethylaminoethyl (**18a**–**18c**) units have favourable ADME properties. However, the low membrane permeability of amidine benzimidazoles suggests further

optimization is required in order to modulate amidine basicity [13,15,60] and, therefore, improve permeability and oral bioavailability.

4. Material and methods

4.1. General

All the solvents and chemicals were purchased from Aldrich and Acros. Thin layer chromatography was performed on pre-coated Merck silica gel 60F-254 plates, while glass column slurry-packed under gravity with silica gel (Fluka, 0.063–0.2 mm) was employed for column chromatography. Melting points of compounds were determined using Kofler micro hot-stage. ^{1}H and ^{13}C NMR spectra were recorded on a Varian Gemini 300 (300 and 75 MHz) or Varian Gemini 600 (600 and 150 MHz). All data were recorded in dimethyl sulfoxide (DMSO-d_6) at 298 K. Chemical shifts were referenced to the residual solvent signal of DMSO at δ 2.50 ppm for ^{1}H and δ 39.50 ppm for ^{13}C. Individual resonances were assigned on the basis of their chemical shifts, signal intensities, multiplicity of resonances, H–H coupling constants and with the use of a set of 2D experiments. High performance liquid chromatography was performed on an Agilent 1100 series system with UV detection (photodiode array detector) using Zorbax C18 reverse-phase analytical column (2.1 × 30 mm, 3.5 μm). All synthesized intermediates **9a**–**13a**, **9b**–**13b** and **9c**–**13c** showed >95% purity in this HPLC system.

4.2. Experimental procedures for the preparation of compounds

4-(Prop-2-ynyloxy)benzaldehyde (**2a**) [61], 3-methoxy-4-(prop-2-ynyloxy) benzaldehyde (**2c**) [62], 4-(imidazolin-2-yl)benzene-1,2-diamine [37], 4-(2-azidoethyl)morpholine [63] were prepared according to known procedure, while compounds 4-(1,2,3-triazol-4-yl)methoxy)benzaldehyde (**3a**) [64], 4-[(1-benzyl-1*H*-1,2,3-triazol-4-yl)methoxy]-3-methoxybenzaldehyde (**3c**) [65], 4-(2-morpholino-2-oxoethoxy)benzaldehyde (**9a**) [66], 3-methoxy-4-(2-morpholino-2-oxoethoxy)benzaldehyde (**9c**) [67], 4-(2-oxo-2-phenylethoxy)benzaldehyde (**10a**) [68], 3-methoxy-4-(2-oxo-2-phenylethoxy)benzaldehyde (**10c**) [69], 4-(pyridin-2-yl-methoxy)benzaldehyde (**11a**) [70], 3-fluoro-4-(pyridin-2-yl-methoxy)benzaldehyde (**11b**) [70], 3-methoxy-4-(piridin-2-yl-methoxy)benzaldehyde (**11c**) [71], 4-(2-morpholinoethoxy)benzaldehyde (**12a**) [72], 3-fluoro-4-(2-morpholinoethoxy)benzaldehyde (**12b**) [73], 3-methoxy-4-(2-morpholinoethoxy)benzaldehyde **(12c)** [74], 4-(2-(diethylamino)ethoxy)benzaldehyde (**13a**) [75], 4-(2-(diethylamino)ethoxy)-3-methoxybenzaldehyde (**13c**) [76], were synthesized according to modified procedures given in the literature.

4.2.1. Preparation of 3-fluoro-4-(prop-2-yn-1-yloxy)benzaldehyde (*2b*)

K_2CO_3 (1.2 eq.) was added to a solution 3-fluoro-4-hydroxybenzaldehyde (5.0 g, 35.7 mmol) in dry ethanol (8–10 mL) and the mixture was stirred for 30 min followed by addition of propargyl bromide (1.2 eq.). The reaction mixture was stirred overnight at reflux temperature. The course of the reaction was monitored by TLC. Upon completion of the reaction, the solvent was evaporated under reduced pressure and the crude residue was purified by column chromatography with CH_2Cl_2. Compound **2b** was obtained as yellow solid (4.5 g, 66%, m. p. = 111–115 °C). ^{1}H NMR (600 MHz, DMSO-d_6) (δ/ppm): 9.88 (1H, d, J = 2.0 Hz, CHO), 7.80 (1H, dd, J = 8.3, 0.9 Hz, Ph), 7.74–7.72 (1H, m, Ph), 7.45 (1H, t, J = 8.3 Hz, Ph), 5.04 (2H, d, J = 2.4 Hz, CH_2), 3.70 (1H, t, J = 2.4 Hz, CCH). ^{13}C NMR (75 MHz, DMSO) δ 190.8 (d, J_{CF} = 1.8 Hz, CHO), 151.8 (d, J_{CF} = 247.6 Hz, Ph-q), 150.2 (Ph-q), 130.4 (d, J_{CF} = 5.1 Hz, Ph-q), 128.0 (d, J_{CF} = 3.1 Hz, Ph), 115.5 (d, J_{CF} = 18.4 Hz, Ph), 115.2 (d, J_{CF} = 1.3 Hz, Ph), 79.5 (CCH), 78.0 (CCH), 56.7 (OCH_2).

4.2.2. General procedure for synthesis of N-1-benzyl-1,2,3-triazole benzaldehydes *3a*–*3c*

A reaction mixture benzyl chloride (1.1 eq.), NaN_3 (0.9 eq.) and Et_3N (1.3 eq.) was dissolved in *t*-BuOH: H_2O = 1 : 1 (4 mL) and stirred for 30 min. The corresponding terminal alkyne (**2a**–**2c**) and $Cu(OAc)_2$ (0.05 eq) were added. The reaction mixture was stirred overnight at room temperature. The solvent was removed under reduced pressure and the crude reaction mixture was purified by column chromatography with CH_2Cl_2.

4.2.2.1. 4-[(1-Benzyl-1H-1,2,3-triazol-4-yl)methoxy]-3-fluorobenzaldehyde (3b). According to the general procedure from compound **2b** (250 mg, 1.40 mmol) compound **3b** was prepared as colourless oil (378.7 mg, 87%). ^{1}H NMR (300 MHz, DMSO-d_6) (δ/ppm): 9.87 (1H, d, J = 2.1 Hz, CHO), 8.35 (1H, s, H5'), 7.81–7.77 (1H, m, Ph), 7,72–7.57 (1H, m, Ph), 7.60 (1H, t, J = 8.3 Hz, Ph), 7.39–7.29 (5H, m, Ph), 5.63 (2H, s, CH_2), 5.37 (2H, s, CH_2). ^{13}C NMR (75 MHz, DMSO-d_6) (δ/ppm): 191.0 (d, J_{CF} = 1.7 Hz, CHO), 151.8 (d, J_{CF} = 247.1 Hz, Ph-q) 151.2 (d, J_{CF} = 10.9 Hz, Ph-q), 141.9 (C4'), 135.9 (Ph-q), 130.0 (d, J_{CF} = 5.0 Hz, Ph-q), 128.9 (Ph), 128.3 (Ph), 128.0 (Ph), 125.3 (C5'), 115.4; (d, J_{CF} = 18.3 Hz, Ph), 115.2 (d, J_{CF} = 1.5 Hz, Ph), 62.3 (OCH_2), 53.0 (CH_2).

4.2.2.2. 4-[(1-Benzyl-1H-1,2,3-triazol-4-yl)methoxy]-3-methoxybenzaldehyde (3c). According to the general procedure from compound **2c** (250 mg, 1.31 mmol) compound **3c** was prepared as colourless oil (345.6 mg; 82%). ^{1}H NMR (600 MHz, DMSO-d_6) (δ/ppm): 9.85 (1H, s, CHO), 8.31 (1H, s, H5'), 7.55 (1H, dd, J = 8.3, 1.9 Hz, Ph), 7.41–7.31 (7H, m, Ph), 5.62 (2H, s, CH_2), 5.26 (2H, s, CH_2), 3.80 (3H, s, OCH_3). ^{13}C NMR (151 MHz, DMSO-d_6) (δ/ppm): 191.4 (CHO), 152.8 (Ph-q), 149.4 (Ph-q), 142.3 (C4'), 135.9 (Ph-q), 123.0 (Ph-q), 128.8 (Ph), 128.2 (Ph), 128.0 (Ph), 125.7 (Ph), 125.0 (C5'), 112.8 (Ph), 109.9 (Ph), 61.8 (OCH_2), 55.5 (CH_3), 52.9 (CH_2).

4.2.3. General procedure for the synthesis of *4a*–*4c*

4-(2-Chloroethyl)morpholine 156 (3.0 g; 16.12 mmol) was dissolved in deionized water (16 mL) and NaN_3 (3.15 g; 48.37 mmol) was added. The reaction mixture was stirred at 80 °C for 16 h. After completion of the reaction, the mixture was cooled and the pH was adjusted to 10 using 1 M KOH aqueous solution. The mixture was extracted with diethyl ether (3 × 50 mL). The organic layer was dried over anhydrous $MgSO_4$, filtered, and the filtrate was evaporated under reduced pressure at room temperature. The unstable azide (600 mg, 3.84 mmol) was immediately used for the click reaction with the corresponding *O*-propargylated benzaldehyde **2a**–**2c** (3.84 mmol) and $Cu(OAc)_2$ (34.9 mg; 0.19 mmol) in methanol (4 mL). The reaction mixture was stirred at reflux temperature overnight. The course of the reaction was monitored by TLC. Upon completion of the reaction, the solvent was evaporated under reduced pressure and the residue was purified by column chromatography on eluent CH_2Cl_2: CH_3OH = 50 : 1.

4.2.3.1. 4-[(1-(2-Morpholinoethyl)-1H-1,2,3-triazol-4-yl]methoxy} benzaldehyde (4a). According to the general procedure from compound **2a** (615.1 mg, 3.84 mmol) compound **4a** was prepared as colourless crystals (1.01 g, 83%, m.p. = 109–113 °C). ^{1}H NMR (300 MHz, DMSO-d_6) (δ/ppm): 9.88 (1H, s, CHO), 8.26 (1H, s, H5'), 7.88 (2H, d, J = 8.8 Hz, Ph), 7.24 (2H, d, J = 8.8 Hz, Ph), 5.29 (2H, s, CH_2), 4.50 (2H, t, J = 6.3 Hz, CH_2CH_2), 3.55–3.47 (4H, m, $CH_{2\text{-morpholine}}$), 2.73 (2H, t, J = 6.3 Hz, CH_2CH_2), 2.44–2.37 (4H, m, $CH_{2\text{-morpholine}}$). ^{13}C NMR (151 MHz, DMSO-d_6) (δ/ppm): 191.3 (CHO),

162.9 (Ph-q), 141.7 (C4'), 131.7 (Ph), 129.9 (Ph-q), 125.1 (C5'), 115.2 (Ph), 66.1 ($CH_{2\text{-morpholine}}$), 61.5 (OCH_2), 57.2 (CH_2CH_2), 52.9 ($CH_{2\text{-morpholine}}$), 46.6 (CH_2CH_2).

4.2.3.2. 3-Fluoro-4-{[1-(2-morpholinoethyl)-1H-1,2,3-triazol-4-yl] methoxy}benzaldehyde (4b). According to the general procedure from compound **2b** (684.1 mg, 3.84 mmol) compound **4b** was prepared as yellow crystals (1.03 g, 80%, m.p. = 89–93 °C). ^{1}H NMR (300 MHz, DMSO-d_6) (δ/ppm): 9.87 (1H, d, J = 1.9 Hz, CHO), 8.29 (1H, s, H5'), 7.79 (1H, d, J = 8.5 Hz, Ph), 7.72–7.67 (1H, m, Ph), 7.61 (1H, t, J = 8.5 Hz, Ph), 5.38 (2H, s, CH_2), 4.50 (2H, t, J = 6.2 Hz, CH_2CH_2), 3.57–3.42 (4H, m, $CH_{2\text{-morpholine}}$), 2.73 (2H, t, J = 6.2 Hz, CH_2CH_2), 2.44–2.32 (4H, m, $CH_{2\text{-morpholine}}$). ^{13}C NMR (75 MHz, DMSO-d_6) (δ/ppm): 190.8 (d, J_{CF} = 1.7 Hz, CHO), 151.7 (d, J_{CF} = 247.0 Hz, Ph-q), 151.1 (d, J_{CF} = 10.8 Hz, Ph-q), 141.2 (C4'), 129.9 (d, J_{CF} = 5.0 Hz, Ph-q), 128.2 (d, J_{CF} = 3.0 Hz, Ph), 125.5 (C5'), 115.3 (d, J_{CF} = 18.3 Hz, Ph), 115.1 (d, J_{CF} = 1.5 Hz, Ph), 66.1 ($CH_{2\text{-morpholine}}$), 62.3 (OCH_2), 57.3 (CH_2CH_2), 52.9 ($CH_{2\text{-morpholine}}$), 46.5 (CH_2CH_2).

4.2.3.3. 3-Methoxy-4-{[1-(2-morpholinoethyl)-1H-1,2,3-triazol-4-yl] methoxy}benzaldehyde (4c). According to the general procedure from compound **2c** (729.8 mg; 3.84 mmol) compound **4c** was prepared as white solid (1.3 g, 98%, m.p. = 142–146 °C). ^{1}H NMR (300 MHz, DMSO-d_6) (δ/ppm): 9.85 (1H, s, CHO), 8.25 (1H, s, H5'), 7.56 (1H, dd, J = 8.2, 1.8 Hz, Ph), 7.45–7.33 (2H, m, Ph), 5.27 (2H, s, CH_2), 4.50 (2H, t, J = 6.3 Hz, CH_2CH_2), 3.81 (3H, s, OCH_3), 3.54–3.49 (4H, m, $CH_{2\text{-morpholine}}$), 2.74 (2H, t, J = 6.3 Hz, CH_2CH_2), 2.44–2.37 (4H, m, $CH_{2\text{-morpholine}}$). ^{13}C NMR (75 MHz, DMSO-d_6) (δ/ppm): 191.3 (CHO), 152.8 (Ph-q), 149.3 (C4'), 141.7 (Ph-q), 129.9 (Ph-q), 125.7 (Ph), 125.3 (C5'), 112.6 (Ph), 109.7 (Ph), 66.0 ($CH_{2\text{-morpholine}}$), 61.7 (OCH_2), 57.3 (CH_2CH_2), 55.5 (OCH_3), 52.9 ($CH_{2\text{-morpholine}}$), 46.5 (CH_2CH_2).

*4.2.4. Preparation of 4-[(1H-1,2,3-triazol-4-yl)methoxy] benzaldehyde (**5**)*

Compound **2a** (400 mg, 2.30 mmol) was dissolved in DMF: MeOH = 9 : 1 (4.60 mL), then $TMSN_3$ (0.45 mL, 3.44 mmol) and CuI (21.9 mg, 0.12 mmol) were added to the reaction mixture and stirred overnight at 100 °C. After completion the reaction, mixture was evaporated to dryness and the crude residue was purified by column chromatography (CH_2Cl_2: CH_3OH = 100 : 1). Compound **5** was obtained as white solid (355.8 mg, 76%, m.p. = 120–123 °C). ^{1}H NMR (300 MHz, DMSO-d_6) (δ/ppm): 15.13 (1H, bs, NH), 9.88 (1H, s, CHO), 8.09–7.99 (1H, m, H5'), 7.88 (2H, d, J = 8.8 Hz, Ph), 7.24 (2H, d, J = 8.8 Hz, Ph), 5.32 (2H, s, CH_2). ^{13}C NMR (75 MHz, DMSO-d_6) (δ/ppm): 191.4 (CHO), 162.9 (Ph-q), 131.8 (Ph), 129.9 (Ph-q), 128.0 (C5'), 115.3 (Ph), 61.2 (CH_2).

*4.2.5. General procedure for the synthesis of benzimidazole derivatives **6a**–**6c** and **8***

The reaction mixture of 4-triazolylbenzaldehyde derivative (**3a**–**3c**, **5**) the corresponding *o*-phenylenediamine and 40% $NaHSO_3$ (aq) was dissolved in EtOH (15 mL) and stirred under reflux for 6–8 h. After completion of the reaction, $NaHSO_3$ was filtered and the reaction mixture was evaporated to dryness. Water was added (5 mL) and the mixture was stirred overnight and filtered. The crude residue was dissolved in HCl saturated EtOH (8–10 mL) and stirred for 4 h. Addition of ether resulted in precipitation of products **6a**–**6c** and **8**. Solid was collected by filtration, washed with anhydrous ether, and dried under vacuum.

4.2.5.1. 2-{4-[(1-Benzyl-1H-1,2,3-triazol-4-yl)methoxy]phenyl}-1H-benzo[d]imidazole (6a). Compound **6a** was prepared using the above described method from **3a** and 1,2-phenylenediamine (55.3 mg, 0.51 mmol) to obtain **6a** as yellow solid (182.3 mg, 94%, m.p. > 250 °C). ^{1}H NMR (600 MHz, DMSO-d_6) (δ/ppm): 8.32 (1H, s, H5'), 8.11 (2H, d, J = 8.8 Hz, Ph), 7.59–7.55 (2H, m, H4; H7), 7.40–7.36 (2H, m, H5; H6), 7.36–7.31 (3H, m, Ph), 7.24–7.17 (4H, m, Ph), 5.63 (2H, s, OCH_2), 5.24 (2H, s, CH_2). ^{13}C NMR (75 MHz, DMSO-d_6) (δ/ppm): 159.4 (Ph-q), 142.7 (C4'), 135.9 (C3/C7a), 128.7 (Ph), 128.1 (Ph), 128.0 (Ph), 127.9 (Ph), 124.7 (C5'), 122.6 (C2), 121.9 (C5/C6), 115.1 (C4/C7), 61.2 (OCH_2), 52.8 (CH_2). Anal. calcd. for $C_{23}H_{19}N_5O$ (M_r = 381.43): C 72.42, H 5.02, N 18.36; found: C 72.16, H 4.81, N 18.63.

4.2.5.2. 2-{4-[(1-Benzyl-1H-1,2,3-triazol-4-yl)methoxy]-3-fluorophenyl}-5-(imidazolin-2-yl)-1H-benzo[d]imidazole hydrochloride (6b). Compound **6b** was prepared using the above described method from **3b** (150 mg, 0.48 mmol) and 4-(imidazolin-2-yl) benzene-1,2-diamine (110.2 mg, 0.48 mmol) to obtain **6b** as white solid (79.5 mg, 35%, m.p. = 200–203 °C). ^{1}H NMR (600 MHz, DMSO-d_6) (δ/ppm): 10.83 (2H, s, CNH), 8.45 (1H, s, H4), 8.38 (1H, s, H5'), 7.99–7.96 (2H, m, Ph), 7.98 (1H, d, J = 8.6 Hz, H7), 7.88 (1H, d, J = 8.6 Hz, H6), 7.65 (1H, t, J = 8.6 Hz, Ph), 7.40–7.36 (2H, m, Ph), 7.35–7.32 (3H, m, Ph), 5.64 (2H, s, OCH_2), 5.37 (2H, s, CH_2), 4.02 (4H, s, $\underline{CH_2CH_2}$). ^{13}C NMR (75 MHz, DMSO-d_6) (δ/ppm): 165.0 (CNH), 151.5 (d, J_{CF} = 244.9 Hz, Ph-q), 152.5 (d, J_{CF} = 2.4 Hz, C2), 148.8 (d, J_{CF} = 10.3 Hz, Ph-q), 142.0 (C4'), 135.9 (C7a/C3a), 128.8 (Ph), 128.2 (Ph), 128.0 (Ph), 125.2 (Ph), 123.6 (C5'), 116.6 (C5), 115.8 (C4/C7), 115.3 (d, J_{CF} = 20.9 Hz, Ph), 62.2 (OCH_2), 52.9 (CH_2), 44.3 ($\underline{CH_2CH_2}$). Anal. calcd. for $C_{26}H_{22}FN_7O \times HCl \times 0.5H_2O$ (M_r = 512.97): C 60.88, H 4.72, N 19.11; found: C 60.63, H 4.41, N 19.22.

4.2.5.3. 2-{4-[(1-Benzyl-1H-1,2,3-triazol-4-yl)methoxy]-3-methoxyphenyl}-5-(imidazolin-2-yl)-1H-benzo[d]imidazole hydrochloride (6c). Compound **6c** was prepared using the above described method from **3c** (150 mg, 0.46 mmol) and 4-(imidazolin-2-yl)benzene-1,2-diamine (106.1 mg, 0.46 mmol) to obtain **6c** as white solid (179.4 mg, 81%, m.p. = 197–200 °C). ^{1}H NMR (600 MHz, DMSO-d_6) (δ/ppm): 10.88 (2H, s, CNH), 8.46 (1H, s, H4), 8.35 (1H, s, H5'), 8.16 (1H, s, Ph), 8.08 (1H, d, J = 8.3 Hz, H6), 8.02 (1H, d, J = 8.3 Hz, H7), 7.92 (1H, d, J = 8.6 Hz, Ph), 7.45 (1H, d, J = 8.6 Hz, Ph), 7.40–7.29 (5H, m, Ph), 5.63 (2H, s, OCH_2), 5.28 (2H, s, CH_2), 4.03 (4H, s, $\underline{CH_2CH_2}$), 3.90 (3H, s, OCH_3). ^{13}C NMR (75 MHz, DMSO-d_6) (δ/ppm): 165.2 (CNH), 153.6 (C2), 151.0 (Ph-q), 149.5 (Ph-q), 142.6 (C4'), 139.6 (C3a/C7a), 136.1 (Ph-q), 129.0 (Ph), 128.5 (Ph), 128.2 (Ph), 125.3 (C6), 124.0 (C5'), 121.5 (Ph), 118.8 (Ph-q), 117.2 (C5), 115.8 (C4), 114.9 (C7), 113.7 (Ph), 111.1 (Ph), 61.9 (OCH_2), 56.1 (OCH_3), 53.1 (CH_2), 44.6 ($\underline{CH_2CH_2}$). Anal. calcd. for $C_{27}H_{25}N_7O_2 \times HCl \times H_2O$ (M_r = 534.01): C 60.73, H 5.28, N 18.36; found: C 60.81, H 5.20 N 18.39.

4.2.5.4. 5-(Imidazolin-2-yl)-2-{4-[(1H-1,2,3-triazol-4-yl)methoxy] phenyl}-1H-benzo[d]imidazole hydrochloride (8). Compound **8** was prepared using the above described method from **5** (150 mg, 0.74 mmol) and 4-(imidazolin-2-yl)benzene-1,2-diamine (168.8 mg, 0.74 mmol) to obtain **8** as white solid (251.5 mg, 94%, m.p. = 229–232 °C). ^{1}H NMR (300 MHz, DMSO-d_6) (δ/ppm): 10.90 (2H, s, CNH), 8.47 (1H, s, H5'), 8.43 (2H, d, J = 8.9 Hz, Ph), 8.07–8.01 (2H, m, H4; H6), 7.94 (1H, d, J = 8.6 Hz, H7), 7.35 (2H, d, J = 8.9 Hz, Ph), 5.35 (2H, s, CH_2), 4.03 (4H, s, $\underline{CH_2CH_2}$). ^{13}C NMR (151 MHz, DMSO-d_6) (δ/ppm): 164.7 (CNH), 161.6 (C2), 152.7 (Ph-q), 130.1 (Ph), 124.4 (C5'), 117.6 (C4), 115.7 (Ph), 115.5 (C7), 114.6 (C6), 61.2 (CH_2), 44.3 ($\underline{CH_2CH_2}$). Anal. calcd. for $C_{19}H_{17}N_7O \times HCl \times 1.5H_2O$ (M_r = 422.87): C 53.97, H 5.01, N 23.19; found: C 53.61, H 4.77, N 23.43.

*4.2.6. General procedure for the synthesis of benzimidazole derivatives **7a**–**7c***

The reaction mixture of the corresponding 4-

triazolylbenzaldehyde derivative (**4a**–**4c**), 4-(imidazolin-2-yl)benzene-1,2-diamine (1 eq) and *p*-benzoquinone (1 eq) was dissolved in EtOH (15 mL) and stirred under reflux for 6–8 h. Addition of ether resulted in precipitation of products **7a**–**7c**. Solid was collected by filtration, washed with anhydrous ether, and dried under vacuum.

4.2.6.1. 5-(Imidazolin-2-yl)-2-{4-[(1-(2-morpholinoethyl)-1H-1,2,3-triazol-4-yl)methoxy]phenyl}-1H-benzo[d]imidazole dihydrochloride (7a). According to the above-mentioned procedure, from compound **3a** (150 mg, 0.47 mmol) compound **7a** was obtained as grey solid (74.5 mg, 33%, m.p. = 207–210 °C). ^{1}H NMR (300 MHz, DMSO-d_6) (δ/ppm): 11.98 (1H, bs, NH), 10.94 (2H, s, CNH), 8.50–8.40 (4H, m, H4; H5'; Ph) 8.04 (1H, dd, J = 8.6, 1.4 Hz, H6), 7.90 (1H, d, J = 8.6 Hz, H7), 7.33 (2H, d, J = 9.0 Hz, Ph), 5.33 (2H, s, OCH_2), 4.98 (2H, t, J = 7.0 Hz, CH_2CH_2), 4.02 (4H, s, $\underline{CH_2}\underline{CH_2}$), 3.97–3.80 (4H, m, $CH_{2\text{-morpholine}}$), 3.69 (2H, t, J = 7.0 Hz, $\overline{CH_2}\overline{CH_2}$), 3.50–3.33 (2H, m, $CH_{2\text{- morpholine}}$), 3.22–3.03 (2H, m, $CH_{2\text{-morpholine}}$). ^{13}C NMR (75 MHz, DMSO-d_6) (δ/ppm): 164.9 (CNH), 161.3 (Ph-q), 153.0 (C2), 142.5 (C4'), 139.1 (Ph-q), 136.5 (C7a), 135.4 (C3a), 129.9 (Ph), 125.5 (C5'), 124.0 (C6), 117.1 (C5), 115.7 (C4), 115.6 (Ph), 114.7 (C7), 63.1 ($CH_{2\text{-morpholine}}$), 61.4 (OCH_2), 54.1 (CH_2CH_2), 51.2 ($CH_{2\text{-morpholine}}$), 44.3 (CH_2CH_2), 43.6 ($\underline{CH_2}\underline{CH_2}$). Anal. calcd. for $C_{25}H_{28}N_8O_2 \times 2HCl \times 1.75H_2O$ (M_r = 576.99): C 52.04, H 5.85, N 19.42; found: C 52.27, H 5.97, N 19.26.

4.2.6.2. 5-(Imidazolin-2-yl)-2-{4-[(1-(2-morpholinoethyl)-1H-1,2,3-triazol-4-yl)methoxy]-3-fluorophenyl}-1H-benzo[d]imidazole dihydrochloride (7b). According to the above-mentioned procedure, from compound **3b** (150 mg, 0.45 mmol) compound **7b** was obtained as brown solid (169.6 mg, 72%, m.p. = 202–206 °C). ^{1}H NMR (300 MHz, DMSO-d_6) (δ/ppm): 14.17–13.55 (1H, m, NH), 10.66 (2H, s, CNH), 8.45–8.26 (2H, m, H5'; H4), 8.20–8.05 (2H, m, Ph; H6), 7.92–7.72 (2H, m, Ph; H7), 7.60 (1H, t, J = 8.6 Hz, Ph), 5.36 (2H, s, OCH_2), 4.52 (2H, t, J = 6.1 Hz, CH_2CH_2), 4.02 (4H, s, $\underline{CH_2}\underline{CH_2}$), 3.60–3.41 (4H, m, $CH_{2\text{-morpholine}}$), 2.75 (2H, t, J = 5.5 Hz, $\overline{CH_2}\overline{CH_2}$), 2.41 (4H, bs, $CH_{2\text{-morpholine}}$). ^{13}C NMR (75 MHz, DMSO-d_6) (δ/ppm): 165.4 (CNH), 153.3 (C2), 151.7 (d, J_{CF} = 244.1 Hz, Ph-q), 148.0 (d, J_{CF} = 6.1 Hz, Ph-q), 141.6 (C4'), 125.4 (C5'), 123.9 (Ph), 122.5 (d, J_{CF} = 7.2 Hz, Ph-q), 115.8 (Ph), 115.7 (C4), 115.3 (C5), 114.6 (d, J_{CF} = 17.3 Hz, Ph), 112.2 (C7), 66.0 ($CH_{2\text{-morpholine}}$), 62.2 (OCH_2), 57.2 (CH_2CH_2), 52.9 ($CH_{2\text{-morpholine}}$), 46.5 (CH_2CH_2), 44.3 ($\underline{CH_2}\underline{CH_2}$). Anal. calcd. for $C_{25}H_{27}FN_8O_2 \times 2HCl \times 2.25H_2O$ (M_r = 603.99): C 49.71, H 5.59, N 18.85; found: C 49.48, H 5.37, N 18.96.

4.2.6.3. 5-(Imidazolin-2-yl)-2-{4-[(1-(2-morpholinoethyl)-1H-1,2,3-triazol-4-yl)methoxy]-3-methoxyphenyl}-1H-benzo[d]imidazole dihydrochloride (7c). According to the above-mentioned procedure, from compound **3c** (150 mg; 0.43 mmol) compound **7c** was obtained as grey solid (184.1 mg, 85%, m.p. = 180–184 °C). ^{1}H NMR (600 MHz, DMSO-d_6) (δ/ppm): 13.94–13.44 (1H, m, NH), 10.60 (2H, m, CNH), 8.42–8.18 (2H, m, H5', H4), 7.98–7.70 (4H, m, Ph; H6; H7), 7.36 (1H, d, J = 8.4 Hz, Ph), 5.24 (2H, s, OCH_2), 4.52 (2H, t, J = 5.6 Hz, CH_2CH_2), 4.02 (4H, s, $\underline{CH_2}\underline{CH_2}$), 3.89 (3H, s, OCH_3), 3.53 (4H, s, $CH_{2\text{-morpholine}}$), 2.75 (2H, s, $\overline{CH_2}\overline{CH_2}$), 2.42 (4H, s, $CH_{2\text{-morpholine}}$). ^{13}C NMR (151 MHz, DMSO-d_6) (δ/ppm): 164.8 (CNH), 153.0 (Ph-q), 150.9 (C5), 149.2 (Ph-q), 142.4 (C4'), 125.5 (Ph), 124.1 (C6), 121.6 (C5'), 117.2 (C5), 115.6 (C4), 113.5 (Ph, C7), 111.4 (Ph), 63.0 ($CH_{2\text{-morpholine}}$), 61.7 (OCH_2), 56.1 (OCH_3), 54.1 (CH_2CH_2), 51.2 ($CH_{2\text{-morpholine}}$), 44.3 (CH_2CH_2), 43.6 ($\underline{CH_2}\underline{CH_2}$). Anal. calcd. for $C_{26}H_{30}N_8O_3 \times 2HCl \times H_2O$ (M_r = 593.51): C 52.62, H 5.77, N 18.88; found: C 52.29.48, H 5.94, N 18.73.

*4.2.7. General procedure for the synthesis of benzaldehydes **9a**–**13a**, **9b**–**13b** and **9c**–**13c***

The corresponding hydroxybenzaldehyde (**1a**–**1c**) was dissolved in dry acetonitrile (15–20 mL) and K_2CO_3 (1.5 eq) was added. The reaction mixture was stirred for 30 min and the appropriate halide (1 eq) was added and stirring was continued overnight at reflux temperature. The course of the reaction was monitored by TLC. After completion of the reaction, the solvent was evaporated under reduced pressure and the residue was purified by column chromatography.

4.2.7.1. 4-(2-Morpholino-2-oxoethoxy)benzaldehyde (9a). Compound **9a** was prepared according to the general procedure from 4-hydroxybenzaldehyde **1a** (250 mg, 2.05 mmol) and *N*-(chloroacetyl)morpholine (0.27 mL, 2.05 mmol). After purification with column chromatography (CH_2Cl_2: CH_3OH = 100 : 1) compound **9a** was obtained as white solid (506.7 mg, 99%, m.p. = 147–150 °C). ^{1}H NMR (300 MHz, DMSO-d_6) (δ/ppm): 9.87 (1H, s, CHO), 7.85 (2H, d, J = 8.8 Hz, Ph), 7.11 (2H, d, J = 8.8 Hz, Ph), 5.01 (2H, s, OCH_2), 3.68–3.52 (4H, m, $CH_{2\text{-morpholine}}$), 3.51–3.40 (4H, m, $CH_{2\text{-morpholine}}$). ^{13}C NMR (75 MHz, DMSO-d_6) (δ/ppm): 191.3 (CHO), 165.4 (CO), 163.1 (Ph-q), 131.6 (Ph), 129.8 (Ph-q), 115.1 (Ph), 66.0 ($CH_{2\text{-morpholine}}$), 65.6 (OCH_2), 44.6 ($CH_{2\text{-morpholine}}$), 41.6 ($CH_{2\text{-morpholine}}$).

4.2.7.2. 3-Fluoro-4-(2-morpholino-2-oxoethoxy)benzaldehyde (9b). Compound **9b** was prepared according to the general procedure from 3-fluoro-4-hydroxybenzaldehyde **1b** (250 mg, 1.78 mmol) and *N*-(chloroacetyl)morpholine (0.23 mL, 1.78 mmol). After purification with column chromatography (CH_2Cl_2: CH_3OH = 50 : 1) compound **9b** was obtained as white solid (473.9 mg, 99%, m.p. = 84–88 °C). ^{1}H NMR (300 MHz, DMSO-d_6) (δ/ppm): 9.86 (1H, d, J = 2.0 Hz, CHO), 7.80–7.67 (2H, m, Ph), 7.28 (1H, t, J = 8.5 Hz, Ph), 5.13 (2H, s, OCH_2), 3.64–3.54 (4H, m, $CH_{2\text{-morpholine}}$), 3.47–3.42 (4H, m, $CH_{2\text{-morpholine}}$). ^{13}C NMR (75 MHz, DMSO-d_6) (δ/ppm): 190.8 (d, J_{CF} = 1.9 Hz, CHO), 165.0 (CO), 151.5 (d, J_{CF} = 247.0 Hz, Ph-q) 151.4 (d, J_{CF} = 10.5 Hz, Ph-q), 129.9 (d, J_{CF} = 5.2 Hz, Ph-q), 127.8 (d, J_{CF} = 2.9 Hz, Ph), 115.4 (d, J_{CF} = 18.3 Hz, Ph), 115.0 (d, J_{CF} = 1.5 Hz), 66.1 ($CH_{2\text{-morpholine}}$), 65.9 (OCH_2), 44.5 ($CH_{2\text{-morpholine}}$), 41.6 ($CH_{2\text{-morpholine}}$).

4.2.7.3. 3-Methoxy-4-(2-morpholino-2-oxoethoxy)benzaldehyde (9c). Compound **9c** was prepared according to the general procedure from 3-methoxy-4-hydroxybenzaldehyde **1c** (250 mg, 1.64 mmol) and *N*-(chloroacetyl)morpholine (0.21 mL, 1.64 mmol). After purification with column chromatography (CH_2Cl_2: CH_3OH = 50 : 1) compound **9c** was obtained as white solid (452.3 mg, 99%, m.p. = 80–85 °C). ^{1}H NMR (300 MHz, DMSO-d_6) (δ/ppm): 9.84 (1H, s, CHO), 7.51 (1H, dd, J = 8.3, 1.9 Hz, Ph), 7.42 (1H, d, J = 1.9 Hz, Ph), 7.06 (1H, d, J = 8.3 Hz, Ph), 5.0 (2H, s, OCH_2), 3.85 (3H, s, OCH_3), 3.71–3.52 (4H, m, $CH_{2\text{-morpholine}}$), 3.50–3.39 (4H, m, $CH_{2\text{-morpholine}}$). ^{13}C NMR (75 MHz, DMSO-d_6) (δ/ppm): 191.4 (CHO), 165.3 (CO), 152.9 (Ph-q), 149.2 (Ph-q), 129.9 (Ph-q), 125.5 (Ph), 112.7 (Ph), 110.0 (Ph), 66.1 (OCH_2, $CH_{2\text{-morpholine}}$), 55.6 (OCH_3), 44.7 ($CH_{2\text{-morpholine}}$), 41.6 ($CH_{2\text{-morpholine}}$).

4.2.7.4. 4-(2-Oxo-2-phenylethoxy)benzaldehyde (10a). Compound **10a** was prepared according to the general procedure from 4-hydroxybenzaldehyde **1a** (250 mg, 2.5 mmol) and 2-bromoacetophenone (352.4 mg, 1.78 mmol). After purification with column chromatography (CH_2Cl_2: CH_3OH = 50 : 1) compound **10a** was obtained as yellow solid (324.7 mg, 71%, m.p. = 81–85 °C). ^{1}H NMR (300 MHz, DMSO-d_6) (δ/ppm): 9.87 (1H, s, CHO), 8.04 (2H, d, J = 7.4 Hz, Ph), 7.86 (2H, d, J = 8.8 Hz, Ph), 7.71 (1H, t, J = 7.4 Hz, Ph), 7.58 (2H, t, J = 7.4 Hz, Ph), 7.17 (2H, d, J = 8.8 Hz, Ph), 5.77 (2H, s,

OCH_2). ^{13}C NMR (151 MHz, DMSO-d_6) (δ/ppm): 193.7 (CO), 191.2 (CHO), 162.9 (Ph-q), 134.2 (Ph-q), 133.8 (Ph), 131.6 (Ph), 129.9 (Ph-q), 128.8 (Ph), 127.8 (Ph), 115.1 (Ph), 70.3 (OCH_2).

4.2.7.5. 3-Fluoro-4-(2-oxo-2-phenylethoxy)benzaldehyde (10b). Compound **10b** was prepared according to the general procedure from 3-fluoro-4-hydroxybenzaldehyde **1b** (250 mg, 1.78 mmol) and 2-bromoacetophenone (322.4 mg, 1.78 mmol). After purification with column chromatography (CH_2Cl_2: CH_3OH = 50 : 1) compound **10b** was obtained as yellow solid (365.9 mg, 72%, m.p. = 115–120 °C). ^1H NMR (300 MHz, DMSO-d_6) (δ/ppm): 9.86 (1H, d, J = 2.0 Hz, CHO), 8.06–7.89 (2H, m, Ph), 7.83–7.65 (3H, m, Ph), 7.59 (2H, t, J = 7.6 Hz, Ph), 7.35 (1H, t, J = 8.5 Hz, Ph), 5.89 (2H, s, OCH_2). ^{13}C NMR (75 MHz, DMSO-d_6) (δ/ppm): 193.4 (CO), 190.8 (d, J_{CF} = 1.8 Hz, CHO), 151.5 (d, J_{CF} = 247.1 Hz, Ph-q), 151.2 (d, J_{CF} = 10.6 Hz, Ph-q), 134.0 (Ph), 130.0 (d, J_{CF} = 5.0 Hz, Ph-q), 128.9 (Ph), 128.0 (Ph), 127.9 (Ph), 115.6 (Ph), 115.3 (d, J_{CF} = 18.3 Hz, Ph), 115.0 (Ph), 70.9 (OCH_2).

4.2.7.6. 3-Methoxy-4-(2-oxo-2-phenylethoxy)benzaldehyde (10c). Compound **10c** was prepared according to the general procedure from 3-methoxy-4-hydroxybenzaldehyde **1c** (250 mg, 1.64 mmol) and 2-bromoacetophenone (324.7 mg, 1.64 mmol). After purification with column chromatography (CH_2Cl_2: CH_3OH = 50 : 1) compound **10c** was obtained as white solid (424.7 mg, 96%, m.p. = 132–134 °C). ^1H NMR (300 MHz, DMSO-d_6) (δ/ppm): 9.84 (1H, s, CHO), 8.03 (2H, d, J = 7.4 Hz, Ph), 7.70 (1H, d, J = 7.4 Hz, Ph), 7.58 (2H, t, J = 7.4 Hz, Ph), 7.52–7.40 (2H, m, Ph), 7.10 (1H, d, J = 8.3 Hz, Ph), 5.77 (2H, s, OCH_2), 3.88 (3H, s, OCH_3). ^{13}C NMR (151 MHz, DMSO-d_6) (δ/ppm): 193.7 (CO), 191.3 (CHO), 152.8 (Ph-q), 149.2 (Ph-q), 134.2 (Ph-q), 133.9 (Ph), 130.0 (Ph-q), 128.8 (Ph), 127.9 (Ph), 125.5 (Ph), 112.7 (Ph), 110.1 (Ph), 70.5 (OCH_2), 55.6 (OCH_3).

4.2.7.7. 4-(Piridin-2-yl-methoxy)benzaldehyde (11a). Compound **11a** was prepared according to the general procedure from 4-hydroxybenzaldehyde **1a** (250 mg, 2.5 mmol) and 2-(chloromethyl)pyridine (403.5 mg, 2.05 mmol). After purification with column chromatography (CH_2Cl_2: CH_3OH = 100 : 1) compound **11a** was obtained as white solid (385.3 mg, 88%, m.p. = 94–97 °C). ^1H NMR (300 MHz, DMSO-d_6) (δ/ppm): 9.87 (1H, s, CHO), 8.59 (1H, d, J = 4.2 Hz, H6'), 7.92–7.80 (3H, m, Ph, H4'), 7.53 (1H, d, J = 7.8 Hz, H3'), 7.36 (1H, dd, J = 6.8, 5.0 Hz, H5'), 7.23 (2H, d, J = 8.7 Hz, Ph), 5.31 (2H, s, OCH_2). ^{13}C NMR (75 MHz, DMSO-d_6) (δ/ppm): 191.3 (CHO), 163.1 (Ph-q), 155.9 (C2'), 149.2 (C6'), 137.1 (Ph), 131.8 (Ph-q), 129.9 (C4'), 123.2 (C3'), 121.9 (C5'), 115.3 (Ph), 70.6 (OCH_2).

4.2.7.8. 3-Fluoro-4-(piridin-2-yl-methoxy)benzaldehyde (11b). Compound **11b** was prepared according to the general procedure from 3-fluoro-4-hydroxybenzaldehyde **1b** (250 mg, 1.78 mmol) and 2-(chloromethyl)pyridine (351.0 mg, 1.78 mmol). After purification with column chromatography (CH_2Cl_2: CH_3OH = 100 : 1) compound **11b** was obtained as white solid (307.6 mg, 75%, m.p. = 82–85 °C). ^1H NMR (300 MHz, DMSO-d_6) (δ/ppm): 9.87 (1H, d, J = 2.1 Hz, CHO), 8.76–8.33 (1H, m, 6′), 7.87 (1H, td, J = 7.7, 1.8 Hz, Ph), 7.80–7.70 (2H, m, Ph, H4'), 7.55 (1H, d, J = 7.8 Hz, H3'), 7.47 (1H, t, J = 8.2 Hz, Ph), 7.41–7.32 (1H, m, H5'), 5.39 (2H, s, OCH_2). ^{13}C NMR (151 MHz, DMSO-d_6) (δ/ppm): 190.8 (CHO), 155.3 (Ph-q, C2') 151.6 (d, J_{CF} = 246.9 Hz, Ph-q), 151.3 (d, J_{CF} = 10.5 Hz, Ph-q), 149.2 (C6'), 137.1 (Ph), 130.0 (d, J_{CF} = 5.1 Hz, Ph-q), 128.2 (C4'), 123.3 (C5'), 121.9 (C5'), 115.4 (d, J_{CF} = 18.2 Hz, Ph), 115.1 (Ph), 71.3 (OCH_2).

4.2.7.9. 3-Methoxy-4-(piridin-2-yl-methoxy)benzaldehyde (11c). Compound **11c** was prepared according to the general procedure from 3-methoxy-4-hydroxybenzaldehyde **1c** (250 mg, 1.64 mmol) and 2-(chloromethyl)pyridine (323.1 mg, 1.64 mmol). After purification with column chromatography (CH_2Cl_2: CH_3OH = 100 : 1) compound **11c** was obtained as white solid (398.7 mg, 60%, m.p. = 77–81 °C). ^1H NMR (300 MHz, DMSO-d_6) (δ/ppm): 9.85 (1H, s, CHO), 8.59 (1H, d, J = 4.2 Hz, H6'), 7.86 (1H, td, J = 7.7, 1.7 Hz, Ph), 7.58–7.48 (2H, m, H4', H3'), 7.44 (1H, d, J = 1.8 Hz, Ph), 7.37 (1H, dd, J = 6.8, 5.1 Hz, H5'), 7.26 (1H, d, J = 8.3 Hz, Ph), 5.29 (2H, s, OCH_2), 3.87 (3H, s, OCH_3). ^{13}C NMR (151 MHz, DMSO-d_6) (δ/ppm): 191.4 (CHO), 155.9 (Ph-q), 152.9 (Ph-q), 149.4 (C2'), 149.2 (C6'), 137.1 (Ph), 130.0 (Ph-q), 125.8 (C4'), 123.2 (C3'), 121.9 (C5'), 112.7 (Ph), 109.9 (Ph), 70.9 (OCH_2), 55.6 (OCH_3).

4.2.7.10. 4-(2-Morpholinoethoxy)benzaldehyde (12a). Compound **12a** was prepared according to the general procedure from 4-hydroxybenzaldehyde **1a** (250 mg, 2.5 mmol) and 4-(2-chloroethyl)morpholine hydrochloride (340 mg, 2.05 mmol). After purification with column chromatography (CH_2Cl_2: CH_3OH = 50 : 1) compound **12a** was obtained as colourless oil (425.2 mg, 88%). ^1H NMR (300 MHz, DMSO-d_6) (δ/ppm): 9.86 (1H, s, CHO), 7.85 (2H, d, J = 8.8 Hz, Ph), 7.13 (2H, d, J = 8.8 Hz, Ph), 4.20 (2H, t, J = 5.7 Hz, CH_2CH_2), 3.70–3.47 (4H, m, $CH_{2\text{-morpholine}}$), 2.71 (2H, t, J = 5.7 Hz, CH_2CH_2), 2.49–2.43 (4H, m, $CH_{2\text{-morpholine}}$). ^{13}C NMR (151 MHz, DMSO-d_6) (δ/ppm): 191.3 (CHO), 163.4 (Ph-q), 131.2 (Ph), 129.6 (Ph-q), 115.0 (Ph), 66.1 ($CH_{2\text{-morpholine}}$), 65.8 (CH_2CH_2), 56.8 (CH_2CH_2), 53.5 ($CH_{2\text{-morpholine}}$).

4.2.7.11. 3-Fluoro-4-(2-morpholinoethoxy)benzaldehyde (12b). Compound **12b** was prepared according to the general procedure from 3-fluoro-4-hydroxybenzaldehyde **1b** (250 mg, 1.78 mmol) and 4-(2-chloroethyl)morpholine hydrochloride (331.2 mg, 1.78 mmol). After purification with column chromatography (CH_2Cl_2: CH_3OH = 50 : 1) compound **12b** was obtained as yellow oil (430.4 mg, 95%). ^1H NMR (300 MHz, DMSO-d_6) (δ/ppm): 9.86 (1H, d, J = 2.1 Hz, CHO), 7.79–7.74 (1H, m, Ph), 7.68 (1H, dd, J = 11.4, 1.9 Hz, Ph), 7.41 (1H, t, J = 8.3 Hz, Ph), 4.29 (2H, t, J = 5.7 Hz, CH_2CH_2), 3.64–3.46 (4H, m, $CH_{2\text{-morpholine}}$), 2.74 (2H, t, J = 5.7 Hz, CH_2CH_2), 2.49–2.43 (4H, m, $CH_{2\text{-morpholine}}$). ^{13}C NMR (75 MHz, DMSO-d_6) (δ/ppm): 190.8 (CHO), 151.6 (d, J_{CF} = 246.9 Hz, Ph-q), 151.7 (d, J_{CF} = 10.7 Hz, Ph-q), 129.7 (d, J_{CF} = 4.9 Hz, Ph-q), 128.3 (d, J_{CF} = 3.1 Hz, Ph), 115.2 (d, J_{CF} = 18.3 Hz, Ph), 114.7 (d, J_{CF} = 1.6 Hz, Ph), 67.0 ($CH_{2\text{-morpholine}}$), 66.1 (CH_2CH_2), 56.6 (CH_2CH_2), 53.5 ($CH_{2\text{-morpholine}}$).

4.2.7.12. 3-Methoxy-4-(2-morpholinoethoxy)benzaldehyde (12c). Compound **12c** was prepared according to the general procedure from 3-methoxy-4-hydroxybenzaldehyde **1c** (250 mg, 1.64 mmol) and 4-(2-chloroethyl)morpholine hydrochloride (305.1 mg, 1.64 mmol). After purification with column chromatography (CH_2Cl_2: CH_3OH = 50 : 1) compound **12c** was obtained as yellow oil (415.9 mg, 96%). ^1H NMR (300 MHz, DMSO-d_6) (δ/ppm): 9.84 (1H, s, CHO), 7.53 (1H, dd, J = 8.3, 1.9 Hz, Ph), 7.39 (1H, d, J = 1.8 Hz, Ph), 7.20 (1H, d, J = 8.3 Hz, Ph), 4.19 (2H, t, J = 5.8 Hz, CH_2CH_2), 3.83 (3H, s, OCH_3), 3.62–3.45 (4H, m, $CH_{2\text{-morpholine}}$), 2.72 (2H, t, J = 5.8 Hz, CH_2CH_2), 2.49–2.43 (4H, m, $CH_{2\text{-morpholine}}$). ^{13}C NMR (75 MHz, DMSO-d_6) (δ/ppm): 191.4 (CHO), 153.4 (Ph-q), 149.3 (Ph-q), 129.7 (Ph-q), 126.0 (Ph), 112.3 (Ph), 109.7 (Ph), 66.4 (CH_2CH_2), 66.2 ($CH_{2\text{-morpholine}}$), 56.8 (CH_2CH_2), 55.6 (OCH_3), 53.6 ($CH_{2\text{-morpholine}}$).

4.2.7.13. 4-(2-(Diethylamino)ethoxy)benzaldehyde (13a). Compound **13a** was prepared according to the general procedure from 4-hydroxybenzaldehyde **1a** (250 mg; 2.5 mmol) and 2-chloro-*N*,*N*-dimethylethylamine hydrochloride (339.4 mg, 2.05 mmol). After purification with column chromatography (CH_2Cl_2: CH_3OH = 50 : 1) compound **13a** was obtained as yellow oil (136.4 mg, 30%). ^1H NMR (300 MHz, DMSO-d_6) (δ/ppm): 9.86 (1H, s,

CHO), 7.85 (2H, d, J = 8.8 Hz, Ph), 7.12 (2H, d, J = 8.8 Hz, Ph), 4.14 (2H, t, J = 5.9 Hz, CH_2CH_2), 2.81 (2H, t, J = 5.9 Hz, CH_2CH_2) 2.62–2.51 (4H, m, $\underline{CH_2}CH_3$), 0.97 (6H, t, J = 7.1 Hz, $CH_2\underline{CH_3}$). ^{13}C NMR (75 MHz, DMSO-d_6) (δ/ppm): 191.8 (CHO), 164.0 (Ph-q), 132.3 (Ph), 130.0 (Ph-q), 115.4 (Ph), 67.3 (CH_2CH_2), 51.6 (CH_2CH_2), 47.4 ($\underline{CH_2}CH_3$), 12.2 ($CH_2\underline{CH_3}$).

4.2.7.14. 4-(2-(Diethiylamino)ethoxy)-3-fluorobenzaldehyde (13b). Compound **13b** was prepared according to the general procedure from 3-fluoro-4-hydroxybenzaldehyde **1b** (250 mg, 1.78 mmol) and 2-chloro-*N*,*N*-dimethylethylamine hydrochloride (295.9 mg, 1.78 mmol). After purification with column chromatography (CH_2Cl_2: CH_3OH = 50 : 1) compound **13b** was obtained as yellow oil (335.1 mg, 79%). ^{1}H NMR (300 MHz, DMSO-d_6) (δ/ppm): 9.82 (1H, d, J = 2.1 Hz, CHO), 7.72 (1H, d, J = 8.5 Hz, Ph), 7.67–7.61 (1H, m, Ph), 7.37 (1H, t, J = 8.5 Hz, Ph), 4.17 (2H, t, J = 5.9 Hz, CH_2CH_2), 2.92–2.70 (2H, m, CH_2CH_2), 2.48–2.41 (4H, m, $\underline{CH_2}CH_3$), 0.93 (6H, t, J = 7.1 Hz, $CH_2\underline{CH_3}$). ^{13}C NMR (151 MHz, DMSO-d_6) (δ/ppm): 190.7 (CHO), 151.6 (d, J_{CF} = 247.0 Hz, Ph-q), 151.8 (d, J_{CF} = 10.7 Hz, Ph-q), 129.6 (d, J_{CF} = 5.1 Hz, Ph-q), 128.2 (d, J_{CF} = 2.7 Hz, Ph), 116.1 (, J_{CF} = 18.3 Hz, Ph), 114.6 (Ph), 67.8 (CH_2CH_2), 50.9 (CH_2CH_2)), 47.0 ($\underline{CH_2}CH_3$), 11.7 ($CH_2\underline{CH_3}$).

4.2.7.15. 4-(2-(Dietihylamino)ethoxy)-3-methoxybenzaldehyde (13c). Compound **13c** was prepared according to the general procedure from 3-methoxy-4-hydroxybenzaldehyde **1c** (250 mg; 1.64 mmol) and 2-chloro-*N*,*N*-dimethylethylamine hydrochloride (272. mg, 1.64 mmol). After purification with column chromatography (CH_2Cl_2: CH_3OH = 50 : 1) compound **13c** was obtained as yellow oil (354.2 mg, 66%). ^{1}H NMR (300 MHz, DMSO-d_6) (δ/ppm): 9.83 (1H, s, CHO), 7.53 (1H, dd, J = 8.3, 1.9 Hz, Ph), 7.39 (1H, d, J = 1.9 Hz, Ph), 7.19 (1H, d, J = 8.3 Hz, Ph), 4.12 (2H, t, J = 6.2 Hz, CH_2CH_2), 3.82 (3H, s, OCH_3), 2.81 (2H, t, J = 6.2 Hz, CH_2CH_2), 2.66–2.50 (4H, m, $\underline{CH_2}CH_3$), 0.97 (6H, t, J = 7.1 Hz, $CH_2\underline{CH_3}$). ^{13}C NMR (75 MHz, DMSO-d_6) (δ/ppm): 191.4 (CHO), 153.5 (Ph-q), 149.3 (Ph-q), 129.6 (Ph-q), 126.1 (Ph), 112.2 (Ph), 109.7 (Ph), 67.3 (CH_2CH_2), 55.6 (OCH_3), 51.1 (CH_2CH_2), 47.0 ($\underline{CH_2}CH_3$), 11.8 ($CH_2\underline{CH_3}$).

*4.2.8. General procedure for the synthesis of benzimidazole derivatives **14a–18a**, **14b–18b** and **14c–18c***

The reaction mixture of the corresponding benzaldehyde derivative (**9a–13a**, **9b–13b**, **9c–13c**), 4-(imidazolin-2-yl)benzene-1,2-diamine (1 eq) and 40% $NaHSO_3$ (aq) was dissolved in 15 mL EtOH and stirred under reflux for 6–8 h. After completion of the reaction $NaHSO_3$ was filtered and the reaction mixture was evaporated to dryness. The crude residue was purified by column chromatography (CH_2Cl_2: CH_3OH = 4 : 1). The obtained solid was dissolved in HCl saturated EtOH (8–10 mL) and stirred for 4 h. Addition of ether resulted in precipitation of products **14a–18a**, **14b–18b** and **14c–18c**. Solid was collected by filtration, washed with anhydrous ether, and dried under vacuum.

4.2.8.1. 5-(Imidazolin-2-yl)-2-[4-(2-morpholino-2-oxoethoxy) phenyl]-1H-benzo[d]imidazole dihydrochloride (14a). According to the above-mentioned procedure, from **9a** (200 mg, 0.80 mmol) compound **14a** was obtained as brown solid (118.6 mg, 37%, m.p. = 220–223 °C). ^{1}H NMR (300 MHz, DMSO-d_6) (δ/ppm): 10.82 (2H, s, CNH), 8.45 (1H, s, H4), 8.39 (2H, d, J = 8.5 Hz, Ph), 8.00 (1H, d, J = 8.3 Hz, H7), 7.89 (1H, d, J = 8.3 Hz, H6), 7.20 (2H, d, J = 8.5 Hz, Ph), 5.01 (2H, s, CH_2), 4.03 (4H, s, $\underline{CH_2}\underline{CH_2}$), 3.73–3.35 (8H, m, CH_2-morpholine). ^{13}C NMR (75 MHz, DMSO-d_6) (δ/ppm): 165.6 (CNH), 165.1 (CO), 161.3 (Ph-q), 153.5 (C2), 129.5 (Ph), 123.7 (C6), 118.9 (C5), 116.8 (Ph-q), 115.9 (C4), 115.5 (Ph), 114.8 (C7), 66.1 (CH_2-morpholine), 65.7 (OCH_2), 44.4 ($\underline{CH_2}\underline{CH_2}$), 44.6 ($CH_2$-morpholine), 41.6 ($CH_2$-morpholine). Anal. calcd. for $C_{22}H_{23}N_5O_3 \times 2HCl \times 2.75H_2O$ (M_r = 527.91): C 50.05, H 5.82, N 13.27; found: C 50.28, H 5.94, N 13.11.

4.2.8.2. 2-[3-Fluoro-4-(2-morpholino-2-oxoethoxy)phenyl]-5-(imidazolin-2-yl)-1H-benzo[d]imidazole dihydrochloride (14b). According to the above-mentioned procedure, from **9b** (200 mg, 0.74 mmol) compound **14b** was obtained as brown solid (265.4 mg, 85%, m.p. = 211–215 °C). ^{1}H NMR (300 MHz, DMSO-d_6) (δ/ppm): 13.87 (1H, s, NH), 10.67 (2H, s, CNH), 8.36 (1H, s, H4), 8.17–8.01 (2H, m, H6, Ph), 7.91–7.72 (2H, m, H7, Ph), 7.29 (1H, t, J = 8.7 Hz, Ph), 5.09 (2H, s, OCH_2), 4.01 (4H, s, $\underline{CH_2}\underline{CH_2}$), 3.69–3.40 (8H, m, CH_2-morpholine). ^{13}C NMR (151 MHz, DMSO-d_6) (δ/ppm): 165.4 (CNH), 165.3 (CO), 151.4 (d, J_{CF} = 244.3 Hz, Ph-q), 149.7 (Ph-q), 148.1 (d, J_{CF} = 10.2 Hz, Ph-q), 123.7 (Ph, C6), 122.4 (d, J_{CF} = 7.1 Hz, Ph-q), 115.6 (C4, Ph), 115.5 (C5), 115.3 (C7), 114.6 (d, J_{CF} = 20.9 Hz, Ph), 66.1 (CH_2-morpholine), 65.9 (OCH_2), 44.6 (CH_2-morpholine), 44.2 ($\underline{CH_2}\underline{CH_2}$), 41.6 ($CH_2$-morpholine). Anal. calcd. for $C_{22}H_{22}FN_5O_3 \times 2HCl \times 3H_2O$ (M_r = 550.41): C 48.01, H 5.49, N 12.72; found: C 47.79, H 5.31, N 13.02.

4.2.8.3. 5-(Imidazolin-2-yl)-2-[3-methoxy-4-(2-morpholino-2-oxoethoxy)phenyl]-1H-benzo[d]imidazole dihydrochloride (14c). According to the above-mentioned procedure, from **9c** (200 mg, 0.72 mmol) compound **14c** was obtained as brown solid (269.7 mg, 86%, m.p. = 202–205 °C). ^{1}H NMR (300 MHz, DMSO-d_6) (δ/ppm): 13.78 (1H, bs, NH), 10.67 (2H, s, CNH), 8.36 (1H, s, H4), 8.00–7.70 (4H, m, Ph; H7; H6), 7.07 (1H, d, J = 8.6 Hz, Ph), 4.94 (2H, s, OCH_2), 4.01 (4H, s, $\underline{CH_2}\underline{CH_2}$), 3.92 (3H, s, OCH_3), 3.73–3.40 (8H, m, CH_2-morpholine). ^{13}C NMR (75 MHz, DMSO-d_6) (δ/ppm): 165.7 (CNH), 165.4 (Ph-q), 149.7 (C2), 149.0 (Ph-q), 122.3 (C6), 122.2 (Ph-q), 119.9 (Ph), 115.6 (C4, C7), 115.0 (Ph-q), 113.4 (Ph), 110.7 (Ph), 66.3 (CH_2-morpholine), 66.0 (OCH_2), 55.9 (OCH_3), 44.8 ($\underline{CH_2}\underline{CH_2}$), 44.2 ($CH_2$-morpholine), 41.6 ($CH_2$-morpholine). Anal. calcd. for $C_{23}H_{25}N_5O_4 \times 2HCl \times 2.25H_2O$ (M_r = 548.93): C 50.32, H 5.78, N 12.76; found: C 50.47, H 5.43, N 13.11.

4.2.8.4. 5-(Imidazolin-2-yl)-2-[4-(2-oxoethoxy-2-phenyl)phenyl]-1H-benzo[d]imidazole hydrochloride (15a). According to the above-mentioned procedure, from **10a** (150 mg, 0.62 mmol) compound **15a** was obtained as brown solid (205 mg, 83%, m.p. = 255–258 °C). ^{1}H NMR (300 MHz, DMSO-d_6) (δ/ppm): 13.67 (1H, s, NH), 10.62 (2H, s, CNH), 8.33 (1H, s, H4), 8.22 (2H, d, J = 8.6 Hz, Ph), 8.06 (2H, d, J = 7.4 Hz, Ph), 7.88–7.65 (3H, m, H6; H7; Ph), 7.59 (2H, t, J = 7.4 Hz, Ph), 7.19 (2H, d, J = 8.6 Hz, Ph), 5.73 (2H, s, OCH_2), 4.01 (4H, s, $\underline{CH_2}\underline{CH_2}$). ^{13}C NMR (75 MHz, DMSO-d_6) (δ/ppm): 194.2 (CO), 165.4 (CNH), 160.1 (C2), 134.3 (Ph-q), 133.9 (Ph), 128.9 (Ph), 128.7 (Ph), 127.9 (Ph), 122.2 (C6), 122.0 (C5), 115.2 (C4, C7), 115.0 (Ph-q), 70.3 (OCH_2), 44.2 ($\underline{CH_2}\underline{CH_2}$). Anal. calcd. for $C_{24}H_{20}N_4O_2 \times HCl \times 2H_2O$ (M_r = 468.93): C 61.47, H 5.37, N 11.95; found: C 61.09, H 4.98, N 12.30.

4.2.8.5. 2-[3-Fluoro-4-(2-oxoethoxy-2-phenyl)phenyl]-5-(imidazolin-2-yl)-1H-benzo[d]imidazole hydrochloride (15b). According to the above-mentioned procedure, from **10b** (150 mg, 0.66 mmol) compound **15b** was obtained as yellow solid (187.2 mg, 68%, m.p. = 205–208 °C). ^{1}H NMR (300 MHz, DMSO-d_6) (δ/ppm): 10.91 (2H, s, CNH), 8.48 (1H, s, H4), 8.39 (1H, dd, J = 12.3, 1.9 Hz, Ph), 8.25 (1H, d, J = 8.8 Hz, H7), 8.09–7.97 (3H, m, Ph; H6), 7.91 (1H, d, J = 8.6 Hz, Ph), 7.72 (1H, t, J = 7.4 Hz, Ph), 7.60 (2H, t, J = 7.4 Hz, Ph), 7.47 (1H, t, J = 8.6 Hz, Ph), 5.90 (2H, s, OCH_2), 4.02 (4H, s, $\underline{CH_2}\underline{CH_2}$). ^{13}C NMR (75 MHz, DMSO-d_6) (δ/ppm): 193.5 (CO), 165.2 (CNH), 152.9 (C2), 151.3 (d, J_{CF} = 238.2 Hz, Ph-q), 148.4 (d, J_{CF} = 10.3 Hz, Ph-q), 134.1 (Ph-q), 133.6 (Ph), 128.6 (Ph), 127.6 (Ph), 124.1 (d, J_{CF} = 1.3 Hz, Ph), 122.9 (C6), 120.9 (Ph-q), 116.3 (C4), 116.0 (C5), 115.6 (C7), 115.0 (d, J_{CF} = 20.9 Hz, Ph), 114.8 (d, J_{CF} = 5.1 Hz, Ph), 70.9 (OCH_2), 44.1 ($\underline{CH_2}\underline{CH_2}$). Anal. calcd. for $C_{24}H_{19}FN_4O_2 \times HCl \times 1.5H_2O$

(M_r = 477.92): C 60.32, H 4.85, N 11.72; found: C 60.03, H 4.98, N 12.07.

4.2.8.6. 2-[3-Fluoro-4-(2-oxoethoxy-2-phenyl)phenyl]-5-(imidazolin-2-yl)-1H-benzo[d]imidazole hydrochloride (15c). According to the above-mentioned procedure, from **10c** (150 mg, 0.55 mmol) compound **15c** was obtained as brown solid (183.6 mg, 78%, m.p. = 206–210 °C). ^{1}H NMR (300 MHz, DMSO-d_6) (δ/ppm): 10.66 (2H, s, CNH), 8.34 (1H, s, H4), 8.05 (2H, d, J = 7.4 Hz, Ph), 7.97–7.67 (5H, m, Ph), 7.59 (2H, t, J = 7.4 Hz, Ph), 7.11 (1H, d, J = 8.6 Hz, Ph), 5.71 (2H, s, OCH_2), 4.01 (4H, s, $\underline{CH_2CH_2}$), 3.95 (3H, s, OCH_3). ^{13}C NMR (75 MHz, DMSO-d_6) (δ/ppm): 194.2 (CO), 165.5 (CNH), 153.7 (C2), 149.7 (Ph-q), 149.0 (Ph-q), 134.3 (Ph-q), 133.9 (Ph), 128.9 (Ph), 127.9 (Ph), 122.3 (Ph), 122.0 (Ph), 120.0 (C6), 115.1 (C5), 113.4 (Ph, C7), 110.7 (Ph), 70.6 (OCH_2), 55.9 (OCH_3), 44.2 ($\underline{CH_2CH_2}$). Anal. calcd. for $C_{25}H_{22}N_4O_3 \times HCl \times 2.25H_2O$ (M_r = 503.46): C 59.64, H 5.51, N 11.13; found: C 60.06, H 5.21, N 11.37.

4.2.8.7. 5-(Imidazolin-2-yl)-2-[4-(pyridin-2-ylmethoxy)phenyl]-1H-benzo[d]imidazole hydrochloride (16a). According to the above-mentioned procedure, from **11a** (150 mg; 0.70 mmol) compound **16a** was obtained as white solid (175.0 mg, 46%, m.p. = 208–211 °C). ^{1}H NMR (600 MHz, DMSO-d_6) (δ/ppm): 11.03 (2H, s, CNH), 8.80 (1H, d, J = 4.9 Hz, H6'), 8.54-8.51 (3H, m, H4, Ph), 8.31-8.22 (1H, m, H4'), 8.14-8.07 (1H, m, H6), 7.92 (1H, d, J = 8.2 Hz, H7), 7.90 (1H, d, J = 7.8 Hz, H3'), 7.73 (1H, dd, J = 7.1, 5.1 Hz, H5'), 7.41 (2H, d, J = 8.8 Hz, Ph), 5.54 (2H, s, OCH_2), 4.03 (4H, s, $\underline{CH_2CH_2}$). ^{13}C NMR (75 MHz, DMSO-d_6) (δ/ppm): 164.8 (CNH), 161.1 (Ph-q), 154.2 (C2'), 152.8 (C2), 146.8 (C6'), 139.7 (Ph), 138.9 (Ph), 135.3 (Ph-q), 129.9 (C4'), 124.0 (C3'), 123.0 (C5'), 118.53, 117.0 (C5), 115.6 (C4), 115.6 (Ph), 114.4 (C7), 69.0 (OCH_2), 44.2 ($\underline{CH_2CH_2}$). Anal. calcd. for $C_{22}H_{19}N_5O \times HCl \times 2H_2O$ (M_r = 441.46): C 59.79, H 5.47, N 15.85; found: C 59.41, H 5.26, N 16.17.

4.2.8.8. 5-(Imidazolin-2-yl)-2-[3-fluoro-4-(pyridin-2-ylmethoxy)phenyl]-1H-benzo[d]imidazole hydrochloride (l6b). According to the above-mentioned procedure, from **11b** (150 mg, 0.65 mmol) compound **16b** was obtained as brown solid (187.2 mg, 74%, m.p. = 200–203 °C). ^{1}H NMR (300 MHz, DMSO-d_6) (δ/ppm): 10.91 (2H, s, CNH), 8.74 (1H, d, J = 4.5 Hz, H6'), 8.48 (1H, s, H4), 8.39 (1H, dd, J = 12.3, 1.9 Hz, H6), 8.28 (1H, d, J = 8.7 Hz, H7), 8.14 (1H, td, J = 7.8, 1.5 Hz, Ph), 8.01 (1H dd, J = 8.5, 1.5 Hz, H4'), 7.88 (1H, d, J = 8.6 Hz, H3'), 7.79 (1H, d, J = 7.9 Hz, Ph), 7.65–7.51 (2H, m, Ph; H5'), 5.52 (2H, s, OCH_2), 4.02 (4H, s, $\underline{CH_2CH_2}$). ^{13}C NMR (75 MHz, DMSO-d_6) (δ/ppm): 165.1 (CNH), 154.9 (C2'), 154.1 (C2), 151.5 (d, J_{CF} = 245.1 Hz, Ph-q),152.7 (C2), 148.7 (d, J_{CF} = 10.5 Hz, Ph-q), 147.4 (C6'), 139.8 (Ph), 136.4 (Ph-q), 124.8 (d, J_{CF} = 3.1 Hz, Ph), 124.6 (C4'), 124.3 (C3'), 123.5 (C6), 123.1 (C5'), 118.2 (C5), 116.8 (C4), 115.8 (C7), 115.4 (d, J_{CF} = 21.2 Hz, Ph), 70.0 (OCH_2), 44.4 ($\underline{CH_2CH_2}$).). Anal. calcd. for $C_{22}H_{18}FN_5O \times HCl \times 1.75H_2O$ (M_r = 455.40): C 58.02, H 4.98, N 15.38; found: C 57.63, H 5.26, N 15.57.

4.2.8.9. 5-(Imidazolin-2-yl)-2-[3-methoxy-4-(pyridin-2-ylmethoxy)phenyl]-1H-benzo[d]imidazole hydrochloride (l6c). According to the above-mentioned procedure, from **11c** (150 mg; 0.62 mmol) compound **16c** was obtained as brown solid (181.7 mg; 73%, m.p. = 265–268 °C). ^{1}H NMR (600 MHz, DMSO-d_6) (δ/ppm): 10.67 (2H, s, CNH), 8.60 (1H, d, J = 4.6 Hz, H6'), 8.35 (1H, s, H4), 7.96 (1H, s, Ph), 7.92–7.81 (3H, m, Ph; H4'; H6), 7.77 (1H, d, J = 8.2 Hz, H7), 7,56 (1H, d, J = 7.9 Hz, H3'), 7.37 (1H, dd, J = 7.2, 5.1 Hz, H5'), 7.24 (1H, d, J = 8.5 Hz, Ph), 5.27 (2H, s, OCH_2), 4.01 (4H, s, $\underline{CH_2CH_2}$), 3.94 (3H, s, OCH_3). ^{13}C NMR (75 MHz, DMSO-d_6) (δ/ppm): 165.4 (CNH), 156.4 (C2), 149.8 (Ph-q), 149.2 (Ph-q), 149.1 (C6'), 137.1 (Ph), 123.1 (C4'), 122.3 (C6), 122.2 (C5), 121.8 (C5'), 120.1 (C3'), 115.1 (Ph-q), 113.4 (C4/C7), 110.6 (Ph), 70.9 (OCH_2), 55.9 (OCH_3), 44.2 ($\underline{CH_2CH_2}$). Anal. calcd. for $C_{23}H_{21}N_5O_2 \times HCl \times 3H_2O$ (M_r = 489.95): C 56.38, H 5.76, N 14.29; found: C 56.03, H 5.39, N 14.57.

4.2.8.10. 5-(Imidazolin-2-yl)-2-[4-(2-morpholinoethoxy)phenyl]1-1H-benzo[d]imidazole hydrochloride (l7a). According to the above-mentioned procedure, from **12a** (150 mg; 0.64 mmol) compound **17a** was obtained as brown solid (248.5 mg, 74%, m.p. = 203–207 °C). ^{1}H NMR (600 MHz, DMSO-d_6) (δ/ppm): 11.82 (1H, s, NH), 10.96 (2H, s, CNH), 8.49–8.44 (3H, m, H4, Ph), 8.04 (1H, dd, J = 8.6, 1.3 Hz, H6), 7.89 (1H, d, J = 8.6 Hz, H7), 7.28 (2H, d, J = 8.9 Hz, Ph), 4.61 (2H, t, J = 5.1 Hz, CH_2CH_2), 4.02 (4H, s, $\underline{CH_2CH_2}$), 3.96–3.87 (6H, m, $CH_{2\text{-morpholine}}$, CH_2CH_2), 3.64–3.40 (4H, m, $CH_{2\text{-morpholine}}$, CH_2CH_2). ^{13}C NMR (151 MHz, DMSO-d_6) (δ/ppm): 165.2 (CNH), 159.6 (Ph-q), 154.0 (C2), 129.0 (Ph), 122.6 (C6), 121.3 (Ph-q), 115.5 (C5), 115.2 (Ph), 115.0 (C4, C7), 62.9 ($CH_{2\text{-morpholine}}$), 62.4 (CH_2CH_2), 54.5 (CH_2CH_2), 51.5 ($CH_{2\text{-morpholine}}$), 44.0 ($\underline{CH_2CH_2}$).

4.2.8.11. 5-(Imidazolin-2-yl)-2-[3-fluoro-4-(2-morpholinoethoxy)phenyl]1-1H-benzo[d]imidazole dihydrochloride (l7b). According to the above-mentioned procedure, from **12b** (150 mg, 0.59 mmol) compound **17b** was obtained as brown solid (301.4 mg, 74%, m.p. = 204–208 °C). ^{1}H NMR (300 MHz, DMSO-d_6) (δ/ppm): 12.00 (1H, bs, NH), 10.99 (2H, s, CNH), 8.50 (1H, s, H4), 8.44–8.25 (2H, m, Ph), 8.04 (1H, dd, J = 8.6, 1.4 Hz, H6), 7.86 (1H, d, J = 8.6 Hz, H7), 7.53 (1H, t, J = 8.7 Hz, Ph), 4.75–4.68 (2H, m, CH_2CH_2), 4.01 (4H, s, $\underline{CH_2CH_2}$), 3.98–3.80 (4H, m, $CH_{2\text{- morpholine}}$), 3.70–3.61 (2H, m, $CH_{2\text{-morpholine}}$), 3.56–3.45 (2H, m, $CH_{2\text{-morpholine}}$) 3.33–3.18 (2H, m, CH_2CH_2). ^{13}C NMR (75 MHz, DMSO-d_6) (δ/ppm): 165.1 (CNH), 151.5 (d, J_{CF} = 244.9 Hz, Ph-q), 152.8 (C2), 147.7 (J_{CF} = 10.0 Hz, Ph-q), 124.3 (J_{CF} = 1.5 Hz, Ph), 122.9 (C6), 121.9 (J_{CF} = 7.5 Hz, Ph-q), 116.5 (C4), 115.8 (C5), 115.7 (Ph), 115.0 (d, J_{CF} = 20.6 Hz, Ph), 114.7 (C7), 63.8 (CH_2CH_2), 62.9 ($CH_{2\text{-morpholine}}$), 54.4 (CH_2CH_2), 51.5 ($CH_{2\text{-morpholine}}$), 44.0 ($\underline{CH_2CH_2}$). Anal. calcd. for $C_{22}H_{24}FN_5O_2 \times 2HCl \times 2.5H_2O$ (M_r = 527.42): C 50.10, H 5.92, N 13.28; found: C 50.03, H 5.71, N 13.72.

4.2.8.12. 5-(Imidazolin-2-yl)-2-[3-methoxy-4-(2-morpholinoethoxy)phenyl]1-1H-benzo[d]imidazole fdihydrochloride (l7c). According to the above-mentioned procedure, from **12c** (150 mg; 0.56 mmol) compound **17c** was obtained as yellow solid (237.7 mg, 87%, m.p. = 217–223 °C). ^{1}H NMR (300 MHz, DMSO-d_6) (δ/ppm): ^{1}H NMR (300 MHz, DMSO) δ 12.08 (1H, bs, NH), 10.97 (2H, s, CNH), 8.50 (1H, s, H4), 8.24 (1H, d, J = 1.8 Hz, Ph), 8.15–8.01 (2H, m, Ph, H6), 7.87 (1H, d, J = 8.6 Hz, H7), 7.31 (1H, d, J = 8.6 Hz, Ph), 4.63 (2H, t, J = 5.1 Hz, CH_2CH_2), 4.02 3H, s, OCH_3), 3.97–3.88 (8H, m, $\underline{CH_2CH_2}$, $CH_{2\text{-morpholine}}$), 3.65–3.40 (4H, m, $CH_{2\text{-morpholine}}$, CH_2CH_2), 3.32–3.20 (2H, m, $CH_{2\text{-morpholine}}$). ^{13}C NMR (151 MHz, DMSO-d_6) (δ/ppm): 165.0 (CNH), 153.3 (C2), 149.8 (Ph-q), 149.4 (Ph-q), 123.3 (Ph), 121.0 (C6), 120.5 (Ph-q), 116.2 (C5), 115.9 (C4), 114.4 (Ph, C7), 111.9 (Ph), 63.6 (CH_2CH_2), 62.8 ($CH_{2\text{-morpholine}}$), 56.2 (OCH_3), 54.5 (CH_2CH_2), 51.5 ($CH_{2\text{-morpholine}}$), 44.0 ($\underline{CH_2CH_2}$). Anal. calcd. for $C_{23}H_{27}N_5O_3 \times 2HCl \times 2H_2O$ (M_r = 530.44): C 52.08, H 6.27, N 13.20; found: C 52.43, H 5.98, N 13.11.

4.2.8.13. 2-{4-[2-(Diethylamino)ethoxy]phenyl}-5-(imidazolin-2-yl)-1H-benzo[d]imidazole dihydrochloride (l8a). According to the above-mentioned procedure, from **13a** (150 mg, 0.68 mmol) compound **18a** was obtained as brown solid (126.8 mg, 49%, m.p. = 214–218 °C). ^{1}H NMR (300 MHz, DMSO-d_6) (δ/ppm): 10.98 (3H, s, CNH), 8.54–8.40 (3H, m, Ph, H4), 8.06 (1H, dd, J = 8.6, 1.3 Hz, H6), 7.90 (1H, d, J = 8.6 Hz, H7), 7.28 (2H, d, J = 8.9 Hz, Ph), 4.56 (2H, t, J = 4.8 Hz, CH_2CH_2), 4.02 (4H, s, $\underline{CH_2CH_2}$), 3.63–3.44 (2H, m, CH_2CH_2), 3.29–3.10 (4H, m, $\underline{CH_2CH_3}$), 1.28 (6H, t, J = 7.2 Hz, $CH_2\underline{CH_3}$). ^{13}C NMR (75 MHz, DMSO-d_6) (δ/ppm): 164.9 (CNH), 160.6 (Ph-q), 153.2 (C2), 129.8 (Ph), 123.9 (C6), 120.5 (Ph-q), 116.8 (C5),

115.4 (Ph), 114.7 (C4, C7), 62.7 (CH_2CH_2), 49.5 (CH_2CH_2), 46.9 ($\underline{CH_2}CH_3$), 44.3 ($\underline{CH_2}CH_2$), 8.4 ($CH_2\underline{CH_3}$). Anal. calcd. for $C_{22}H_{27}N_5O \times 2HCl \times 3H_2O$ ($M_r = 504.45$): C 52.38, H 6.99, N 13.88; found: C 52.21, H 6.58, N 14.12.

4.2.8.14. 2-{4-[2-(Diethylamino)ethoxy]-3-fluorophenyl}-5-(imidazolin-2-yl)-1H-benzo[d]imidazole dihydrochloride (l8b). According to the above-mentioned procedure, from **13b** (150 mg; 0.63 mmol) compound **18b** was obtained as brown solid (157. mg; 63%, m.p. = 205–207 °C). ^{1}H NMR (300 MHz, DMSO-d_6) (δ/ppm): 11.00 (1H, bs, NH), 10.90 (2H, s, CNH), 8.48 (1H, s, H4), 8.40–8.26 (2H, m, Ph), 8.00 (1H, dd, $J = 8.6$, 1.5 Hz, H6), 7.87 (1H, d, $J = 8.6$ Hz, H7), 7.52 (1H, t, $J = 8.7$ Hz, Ph), 4.64 (2H, t, $J = 4.8$ Hz, CH_2CH_2), 4.02 (4H, s, $\underline{CH_2}\underline{CH_2}$), 3.67–3.52 (2H, m, CH_2CH_2), 3.32–3.14 (4H, m, $\underline{CH_2}CH_3$), 1.28 (6H, t, $J = 7.2$ Hz, $CH_2\underline{CH_3}$). ^{13}C NMR (75 MHz, DMSO-d_6) (δ/ppm): 165.1 (CNH), 151.5 (d, $J_{CF} = 245.0$ Hz, Ph-q), 152.7 (C2), 148.2 (d, $J_{CF} = 10.7$ Hz, Ph-q), 124.8 ($J_{CF} = 1.2$ Hz, Ph), 123.4 (C6), 121.1 (d, $J_{CF} = 7.5$ Hz, Ph-q), 116.5 (C4), 116.4 (C5), 115.5 (Ph), 115.2 (d, $J_{CF} = 20.7$ Hz, Ph), 115.0 (C7), 63.9 (CH_2CH_2), 49.5 (CH_2CH_2), 47.3 ($\underline{CH_2}CH_3$), 44.3 ($\underline{CH_2}\underline{CH_2}$), 8.5 ($CH_2\underline{CH_3}$). Anal. calcd. for $C_{22}H_{26}FN_5O \times 2HCl \times 1.5H_2O$ ($M_r = 495.42$): C 53.34, H 6.31, N 14.14; found: C 53.70, H 6.11, N 14.27.

4.2.8.15. 2-{4-[2-(Diethylamino)ethoxy]-3-methoxyphenyl}-5-(imidazolin-2-yl)-1H-benzo[d]imidazole dihydrochloride (l8c). According to the above-mentioned procedure, from **13c** (150 mg, 0.60 mmol) compound **18b** was obtained as yellow solid (183 mg, 75%, m.p. = 227–229 °C). ^{1}H NMR (300 MHz, DMSO-d_6) (δ/ppm): 10.92 (1H, bs, NH), 10.78 (2H, s, CNH), 8.43 (1H, d, $J = 1.0$ Hz, 4H), 8.12 (1H, d, $J = 1.7$ Hz, Ph), 8.01 (1H, dd, $J = 8.5$, 1.7 Hz, Ph), 7.95 (1H, dd, $J = 8.6$, 1.5 Hz, H6), 7.83 (1H, d, $J = 8.6$ Hz, H7), 7.27 (1H, d, $J = 8.5$ Hz, Ph), 4.62–4.36 (2H, m, CH_2CH_2), 4.03 (4H, s, $\underline{CH_2}\underline{CH_2}$), 3.96 (3H, s, OCH_3), 3.59–3.38 (2H, m, CH_2CH_2), 3.32–3.20 (4H, m, $\underline{CH_2}CH_3$), 1.30 (6H, t, $J = 7.2$ Hz, $CH_2\underline{CH_3}$). ^{13}C NMR (75 MHz, DMSO-d_6) (δ/ppm): 165.1 (CNH), 153.6 (C2), 149.3 (Ph-q), 123.0 (Ph), 120.8 (C6), 117.3 (C5), 115.9 (C4), 114.5 (C7), 113.9 (Ph), 111.5 (Ph), 63.5 (CH_2CH_2), 56.2 (OCH_3), 49.5 (CH_2CH_2), 47.1 ($\underline{CH_2}CH_3$), 44.1 ($\underline{CH_2}\underline{CH_2}$), 8.3 ($CH_2\underline{CH_3}$). Anal. calcd. for $C_{23}H_{29}N_5O_2 \times 2HCl \times 2H_2O$ ($M_r = 516.46$): C 53.49, H 6.83, N 13.56; found: C 53.11, H 6.33, N 13.89.

4.3. Antitrypanosomal screening and cytotoxicity assays

4.3.1. Antitrypanosomal screening

Bloodstream form *T. b. brucei* (strain 221) were cultured in modified Iscove's medium [77] and assays were carried out in 96-well microtiter plates (200 μl volumes) to determine theIC_{50} and IC_{90} values of each compound. Parasites growth was initiated at 2.5×10^4 mL^{-1}, compounds were added at range of concentrations, and the plates incubated at 37 °C. Resazurin (20 μl at 0.125 mg mL^{-1}) was added after 48 h, the plates incubated for a further 16 h, and then read in a Spectramax plate reader and data analysed using GraphPad Prism. Each drug was tested in triplicate.

4.3.2. L6 cell proliferation

For cytotoxicity assays, L6 cells (a rat myoblast line) were seeded into 96-well microtiter plates at 1×10^4 mL^{-1} in 200 μL of growth medium, and different compound concentrations were added. The plates were then incubated for 6 days at 37 °C and 20 μL resazurin added to each well. After further 8 h incubation, the fluorescence was determined using a Spectramax plate reader, as outlined above.

4.4. DNA and RNA binding study

Evaluated compounds were dissolved in redistilled water. Those solutions were used for measurements in aqueous buffer (pH = 7, sodium cacodylate buffer, $I = 0.05$ mol dm^{-3}). Polynucleotides were purchased as noted: poly A–poly U, poly $(dAdT)_2$, poly $(dGdC)_2$ and calf thymus ctDNA (Sigma-Aldrich). Polynucleotides were dissolved in Na-cacodylate buffer, $I = 0.05$ mol dm^{-3}, pH = 7. The calf thymus ctDNA was additionally sonicated and filtered through a 0.45 mm filter [78]. Polynucleotide concentration was determined spectroscopically [79,80] as the concentration of phosphates.

4.4.1. UV/Vis measurements

The UV/Vis spectra were recorded on a Varian Cary 100 Bio spectrophotometer using 1 cm path quartz cuvettes. Calibration experiments (SI) were performed at 25 °C and pH = 7 ($I = 0.05$ mol dm^{-3}, sodium cacodylate buffer). Thermal melting curves for DNA, RNA and their complexes with studied compounds were determined as previously described by following the absorption change at 260 nm as a function of temperature. The concentration of the compound solution in thermal melting experiments was 2.2×10^{-5} mol dm^{-3} and the concentration of polynucleotide solution was 6.6×10^{-6} mol dm^{-3}. The absorbance of the ligands was subtracted from every curve and the absorbance scale was normalized. T_m values are the midpoints of the transition curves determined from the maximum of the first derivative and checked graphically by the tangent method. The ΔT_m values were calculated subtracting T_m of the free nucleic acid from T_m of the complex. Every ΔT_m value here reported was the average of at least two measurements. The error in ΔT_m is ±0.5 °C.

4.4.2. Fluorimetric measurements

Fluorescence spectra were recorded on a Varian Cary Eclipse spectrophotometer at 25 °C using appropriate 1 cm path quartz cuvettes. Fluorimetric experiments were performed at pH = 7 ($I = 0.05$ mol dm^{-3}, sodium cacodylate buffer) by adding portions (3×0.7; 3×1.4; 2×2.8; 2×5.6 μL) of polynucleotide solution ($c = 2.9 \times 10^{-3}$ mol dm^{-3}) into the solution of the studied compound ($c = 1.0 \times 10^{-6}$ mol dm^{-3}). In fluorimetric experiments excitation wavelength of $\lambda_{exc} = 317$ and 320 nm was used to avoid the inner filter effect caused due to increasing absorbance of the polynucleotide. Emission was collected in the range $\lambda_{em} = 330$–700 nm. Values for K_s obtained by processing titration data using the Scatchard equation [43], all have satisfactory correlation coefficients (>0.99).

4.4.3. CD measurements

CD spectra were recorded on JASCO J815 spectrophotometer in 1 cm path quartz cuvettes. CD parameters: range = 500-220 nm, data pitch = 2, standard sensitivity, scanning speed = 200 nm/min, accumulation = 3-5. Titrations were performed at the temperature of 25 °C and pH = 7 ($I = 0.05$ mol dm^{-3}, sodium cacodylate buffer). CD experiments were done by adding portions (5×1.2 μL) of compound stock solution ($c = 5.0 \times 10^{-3}$ mol dm^{-3}) into the solution of polynucleotide ($c = 3.0 \times 10^{-5}$ mol dm^{-3}).

4.5. Computational methods

Known inhibitors are retrieved from Chembl. Available X-ray structures of DNA complexes with small ligands were downloaded from the Protein data bank [51]. The ligand docking studies were carried out using Glide docking protocol with standard precision (SP) [81–84] within Schrödinger suite of software [85]. As an X-ray template of AT-rich DNA pdb: 2B0K structure was used while for selectivity investigation, ctDNA from pdb: 6EL8 was selected. Binding poses were refined and binding energy was estimated using MM-GBSA [86–88] protocol and OPLS3 force-field with flexible residues distance being 5 Å. Molecular dynamic simulations

were carried out using Desmond software within the Schroedinger package [89–91]. Simulations were carried out at the room temperature for 20 ns. *In silico* ADME properties as well as structural parameters were calculated by ACD Percepta software [92].

4.6. In vitro ADME profiling

4.6.1. MDCKII-MDR1 permeability assay

MDCKII-hMDR1 cells were obtained from Solvo Biotechnology, Hungary. DMEM, Fetal bovine serum, Glutamax-100, Antibiotic/Antimycotic, DMSO, Dulbecco's phosphate buffer saline, MEM Non-essential amino acids were purchased from Sigma (St. Louis, MO, USA). Bi-directional permeability and *P*-glycoprotein substrate assessment were investigated in Madin-Darby canine epithelial cells with over-expressed human MDR1 gene (MDCKII-MDR1), coding for *P*-glycoprotein. Experimental procedures, as well as cell culture conditions, were the same as previously described [93]. Briefly, compounds (10 μM, 1% DMSO v/v) in duplicate were incubated at 37 °C for 60 min with cell monolayer on 24-well Millicell inserts (Millipore, Burlington, MA, USA) without and with the *P*-glycoprotein inhibitor Elacridar (2 μM, International Laboratory, USA). Inhibition of *P*-glycoprotein was verified by amprenavir (Moravek Biochemicals Inc, Brea, CA, USA) and monolayer integrity by Lucifer yellow (Sigma, St. Louis, MO, USA). Compound concentrations were measured by LC-MS/MS and Lucifer yellow was measured on an Infinite F500 (Tecan, Männedorf, CH) using excitation of 485 nm and emission of 530 nm.

4.6.2. Metabolic stability

Mouse liver microsomes were obtained from Corning Life Sciences (Corning, USA). DMSO, nicotinamide adenine dinucleotide phosphate (NADP), glucose-6-phosphate, glucose-6-phosphate dehydrogenase, magnesium chloride, propranolol, caffeine, diclofenac, phosphate buffer saline (PBS) were purchased from Sigma (St. Louis, MO, USA). Acetonitrile (ACN) and methanol (MeOH) were obtained from Merck (Darmstadt, Germany). Testosterone was purchased from Steraloids (Newport, RI, USA). Metabolic stability was assessed in mouse liver microsomes. Compounds (final concentration of 1 μM, 0.03% DMSO v/v) were incubated in duplicate in phosphate buffer (50 mM, pH 7.4) at 37 °C together with mouse liver microsomes in the absence and presence of the NADPH cofactor (0.5 mM nicotinamide adenine dinucleotide phosphate, 5 mM glucose-6-phosphate, 1.5 U/mL glucose-6-phosphate dehydrogenase and 0.5 mM magnesium chloride). Incubation and sampling was performed on a Freedom EVO 200 (Tecan, Männedorf, CH) at 0.3, 10, 20, 30, 45 and 60 min. The reaction was quenched using 3 vol of a mixture of ACN/MeOH (2:1) containing internal standard (diclofenac), centrifuged and supernatants were analysed using LC-MS/MS.

Metabolic activity of microsomes was verified by simultaneous analysis of several controls including testosterone, propranolol and caffeine. The *in vitro* half-life ($t_{1/2}$) was calculated using GraphPad Prism non-linear regression of % parent compound remaining versus time. In vitro clearance, expressed as μL/min/mg, was estimated from the *in vitro* half-life ($t_{1/2}$), and normalized for the protein amount in the incubation mixture and assuming 52.5 mg of protein per gram of liver.

4.6.3. LC-MS/MS analysis

All samples were quantified using tandem mass spectrometry coupled to liquid chromatography. Samples were analysed on a Sciex API4000 Triple Quadrupole Mass Spectrometer (Sciex, Division of MDS Inc., Toronto, Canada) coupled to a Shimadzu Nexera X2 UHPLC frontend (Kyto, Japan). Samples were injected onto a UHPLC column (HALO2 C18, 2.1 × 20 mm, 2 μm or Luna Omega 1.6 μm Polar C18 100A, 30 × 2.1 mm) and eluted with a gradient at 50 °C. The mobile phase was composed of acetonitrile/water mixture (9/1, with 0.1% formic acid) and 0.1% formic acid in deionized water. The flow rate was 0.7 mL/min and under gradient conditions, leading to a total run time of 1.5–2 min. Positive ion mode with turbo spray, an ion source temperature of 550 °C and a dwell time of 150 ms were utilized for mass spectrometric detection. Quantitation was performed using multiple reaction monitoring (MRM) at the specific transitions for each compound.

Declaration of competing interest

The authors declare that they have no known competing financial interests or personal relationships that could have appeared to influence the work reported in this paper.

Acknowledgment

We greatly appreciate the financial support of the Croatian Science Foundation (projects No. IP-2018-01-4682 and No. IP-2018-01-4694).

Appendix A. Supplementary data

Supplementary data to this article can be found online at https://doi.org/10.1016/j.ejmech.2020.112802.

References

[1] H.P. de Koning, The drugs of sleeping sickness: their mechanisms of action and resistance, and a brief history, Trav. Med. Infect. Dis. 5 (2020) 14–37, https://doi.org/10.3390/tropicalmed5010014.
[2] T. Von Geldern, M.O. Harhay, I. Scandale, R. Don, Kinetoplastid parasites, Top. Med. Chem. 7 (2011) 181–242, https://doi.org/10.1007/7355_2011_17.
[3] E.D. Deeks, Fexinidazole: first global approval, Drugs 79 (2019) 215–220, https://doi.org/10.1007/s40265-019-1051-6.
[4] E. Torreele, B.B. Trunz, D. Tweats, M. Kaiser, R. Brun, G. Mazué, M.A. Bray, B. Pécoul, Fexinidazole - a new oral nitroimidazole drug candidate entering clinical development for the treatment of sleeping sickness, PLoS Neglected Trop. Dis. 4 (2010) e923, https://doi.org/10.1371/journal.pntd.0000923.
[5] H. Burrell-Saward, A.J. Harris, R. de LaFlor, H. Sallam, M.S. Alavijeh, T.H. Ward, S.L. Croft, Dose-dependent effect and pharmacokinetics of fexinidazole and its metabolites in a mouse model of human African trypanosomiasis, Int. J. Antimicrob. Agents 50 (2017) 203–209, https://doi.org/10.1016/j.ijantimicag.2017.01.038.
[6] R.T. Jacobs, B. Nare, S.A. Wring, M.D. Orr, D. Chen, J.M. Sligar, M.X. Jenks, R.A. Noe, T.S. Bowling, L.T. Mercer, C. Rewerts, E. Gaukel, J. Owens, R. Parham, R. Randolph, B. Beaudet, C.J. Bacchi, N. Yarlett, J.J. Plattner, Y. Freund, C. Ding, T. Akama, Y.K. Zhang, R. Brun, M. Kaiser, I. Scandale, R. Don, Scyx-7158, an orally-active benzoxaborole for the treatment of stage 2 human african trypanosomiasis, PLoS Neglected Trop. Dis. 5 (2011) e1151, https://doi.org/10.1371/journal.pntd.0001151.
[7] G. Eperon, M. Balasegaram, J. Potet, C. Mowbray, O. Valverde, F. Chappuis, Treatment options for second-stage gambiense human African trypanosomiasis, Expert Rev. Anti Infect. Ther. 12 (2014) 1407–1417, https://doi.org/10.1586/14787210.2014.959496.
[8] F. Doua, T.W. Miezan, J.R. Sanon Singaro, F. Boa Yapo, T. Baltz, The efficacy of pentamidine in the treatment of early-late stage Trypanosoma brucei gambiense trypanosomiasis, Am. I. Trop. Med. Hyg. 55 (1996) 586–588, https://doi.org/10.4269/ajtmh.1996.55.586.
[9] G.N. Sekhar, A.R. Georgian, L. Sanderson, G. Vizcay-Barrena, R.C. Brown, P. Muresan, R.A. Fleck, S.A. Thomas, Organic cation transporter 1 (OCT1) is involved in pentamidine transport at the human and mouse blood-brain barrier (BBB), PloS One 12 (2017), e0173474, https://doi.org/10.1371/journal.pone.0173474.
[10] T. Wenzler, D.W. Boykin, M.A. Ismail, J.E. Hall, R.R. Tidwell, R. Brun, New treatment option for second-stage African sleeping sickness: in vitro and in vivo efficacy of aza analogs of DB289, Antimicrob. Agents Chemother. 53 (2009) 4185–4192, https://doi.org/10.1128/AAC.00225-09.
[11] C.P. Ward, P.E. Wong, R.J. Burchmore, H.P. De Koning, M.P. Barrett, Trypanocidal furamidine analogues: influence of pyridine nitrogens on trypanocidal activity, transport kinetics, and resistance patterns, Antimicrob. Agents Chemother. 55 (2011) 2352–2361, https://doi.org/10.1128/AAC.01551-10.
[12] M.N.C. Soeiro, E.M. De Souza, C.E. Stephens, D.W. Boykin, Aromatic diamidines as antiparasitic agents, Expet Opin. Invest. Drugs 14 (2005) 957–972, https://doi.org/10.1517/13543784.14.8.957.

[13] M.N.C. Soeiro, K. Werbovetz, D.W. Boykin, W.D. Wilson, M.Z. Wang, A. Hemphill, Novel amidines and analogues as promising agents against intracellular parasites: a systematic review, Parasitology 140 (2013) 929–951, https://doi.org/10.1017/S0031182013000292.
[14] J.C. Munday, L. Settimo, H.P. de Koning, Transport proteins determine drug sensitivity and resistance in a protozoan parasite, Trypanosoma brucei, Front. Pharmacol. 6 (2015) 32–42, https://doi.org/10.3389/fphar.2015.00032.
[15] C.H. Ríos Martínez, J.J. Nué Martínez, G.U. Ebiloma, H.P. De Koning, I. Alkorta, C. Dardonville, Lowering the pKa of a bisimidazoline lead with halogen atoms results in improved activity and selectivity against Trypanosoma brucei in vitro, Eur. J. Med. Chem. 101 (2015) 806–817, https://doi.org/10.1016/j.ejmech.2015.07.013.
[16] R.R. Tidwell, D.W. Boykin, Dicationic DNA minor groove binders as antimicrobial agents, in: M. Demeunynck, C. Bailly, W.D. Wilson (Eds.), Small Molecule DNA RNA Binders from Synthesis to Nucleic Acid Complexes, second ed., Wiley-VCH Verlag GmbH & Co. KGaA, Weinheim, 2002, pp. 414–460, https://doi.org/10.1002/3527601783.
[17] B.J. Fennell, J.A. Naughton, J. Barlow, G. Brennan, I. Fairweather, E. Hoey, N. McFerran, A. Trudgett, A. Bell, Microtubules as antiparasitic drug targets, Expert Opin, Drug Discov 3 (2008) 501–518, https://doi.org/10.1517/17460441.3.5.501.
[18] R. Docampo, S. Moreno, The acidocalcisome as a target for chemotherapeutic agents in Protozoan parasites, Curr. Pharmaceut. Des. 14 (2008) 882–888, https://doi.org/10.2174/138161208784041079.
[19] M.N.C. Soeiro, S.L. De Castro, Trypanosoma cruzi targets for new chemotherapeutic approaches, Expert Opin. Ther. Targets 13 (2009) 105–121, https://doi.org/10.1517/14728220802623881.
[20] M. Munde, M. Lee, S. Neidle, R. Arafa, D.W. Boykin, Y. Liu, C. Bailly, W.D. Wilson, Induced fit conformational changes of a "reversed amidine" heterocycle: optimized interactions in a DNA minor groove complex, J. Am. Chem. Soc. 129 (2007) 5688–5698, https://doi.org/10.1021/ja069003n.
[21] C.R. Millan, F.J. Acosta-Reyes, L. Lagartera, G.U. Ebiloma, L. Lemgruber, J.J. Nué Martínez, N. Saperas, C. Dardonville, H.P. de Koning, J.L. Campos, Functional and structural analysis of AT-specific minor groove binders that disrupt DNA-protein interactions and cause disintegration of the Trypanosoma brucei kinetoplast, Nucleic Acids Res. 45 (2017) 8378–8391, https://doi.org/10.1093/nar/gkx521.
[22] S.K. Andreassend, S.J. Bentley, G.L. Blatch, A. Boshoff, R.A. Keyzers, Screening for small molecule modulators of trypanosoma brucei Hsp70 chaperone activity based upon alcyonarian coral-derived natural products, Mar. Drugs 18 (2020) e81, https://doi.org/10.3390/md18020081.
[23] S. Khare, A.S. Nagle, A. Biggart, Y.H. Lai, F. Liang, L.C. Davis, S.W. Barnes, C.J.N. Mathison, E. Myburgh, M.Y. Gao, J.R. Gillespie, X. Liu, J.L. Tan, M. Stinson, I.C. Rivera, J. Ballard, V. Yeh, T. Groessl, G. Federe, H.X.Y. Koh, J.D. Venable, B. Bursulaya, M. Shapiro, P.K. Mishra, G. Spraggon, A. Brock, J.C. Mottram, F.S. Buckner, S.P.S. Rao, B.G. Wen, J.R. Walker, T. Tuntland, V. Molteni, R.J. Glynne, F. Supek, Proteasome inhibition for treatment of leishmaniasis, Chagas disease and sleeping sickness, Nature 537 (2016) 229–233, https://doi.org/10.1038/nature19339.
[24] F.N. Penas, D. Carta, Á.C. Cevey, M.J. Rada, A.V. Pieralisi, M.G. Ferlin, M.E. Sales, G.A. Mirkin, N.B. Goren, Pyridinecarboxylic acid derivative stimulates pro-angiogenic mediators by PI3K/AKT/mTOR and inhibits reactive nitrogen and oxygen species and NF-κB activation through a PPARγ-dependent pathway in T. Cruzi-Infected macrophages, Front. Immunol. 10 (2020) 2955, https://doi.org/10.3389/fimmu.2019.02955.
[25] A.B. Popov, I. Stolić, L. Krstulović, M.C. Taylor, J.M. Kelly, S. Tomić, L. Tumir, M. Bajić, S. Raić-Malić, Novel symmetric bis-benzimidazoles: synthesis, DNA/RNA binding and antitrypanosomal activity, Eur. J. Med. Chem. 173 (2019) 63–75, https://doi.org/10.1016/j.ejmech.2019.04.007.
[26] A. Bistrović, L. Krstulović, I. Stolić, D. Drenjančević, J. Talapko, M.C. Taylor, J.M. Kelly, M. Bajić, S. Raić-Malić, Synthesis, anti-bacterial and anti-protozoal activities of amidinobenzimidazole derivatives and their interactions with DNA and RNA, J. Enzym. Inhib. Med. Chem. 33 (2018) 271–285, https://doi.org/10.1080/14756366.2018.1484733.
[27] R.M.B.M. Girard, M. Crispim, I. Stolić, F.S. Damasceno, M.S. Da Silva, E.M.F. Pral, M.C. Elias, M. Bajić, A.M. Silber, An aromatic diamidine that targets kinetoplast DNA, impairs the cell cycle in trypanosoma cruzi, and diminishes trypomastigote release from infected mammalian host cells, Antimicrob. Agents Chemother. 60 (2016) 5867–5877, https://doi.org/10.1128/AAC.01595-15.
[28] G.E. Miana, S.R. Ribone, D.M.A. Vera, M. Sánchez-Moreno, M.R. Mazzieri, M.A. Quevedo, Design, synthesis and molecular docking studies of novel N-arylsulfonyl-benzimidazoles with anti Trypanosoma cruzi activity, Eur. J. Med. Chem. 165 (2019) 1–10, https://doi.org/10.1016/j.ejmech.2019.01.013.
[29] A.A. Farahat, M.A. Ismail, A. Kumar, T. Wenzler, R. Brun, A. Paul, W.D. Wilson, D.W. Boykin, Indole and benzimidazole bichalcophenes: synthesis, DNA binding and antiparasitic activity, Eur. J. Med. Chem. 143 (2018) 1590–1596, https://doi.org/10.1016/j.ejmech.2017.10.056.
[30] S. Melchor-Doncel de la Torre, C. Vázquez, Z. González-Chávez, L. Yépez-Mulia, R. Nieto-Meneses, R. Jasso-Chávez, E. Saavedra, F. Hernández-Luis, Synthesis and biological evaluation of 2-methyl-1H-benzimidazole-5-carbohydrazides derivatives as modifiers of redox homeostasis of Trypanosoma cruzi, Bioorg. Med. Chem. Lett 27 (2017) 3403–3407, https://doi.org/10.1016/j.bmcl.2017.06.013.
[31] S. Oh, S. Kim, S. Kong, G. Yang, N. Lee, D. Han, J. Goo, J.L. Siqueira-Neto, L.H. Freitas-Junior, R. Song, Synthesis and biological evaluation of 2,3-dihydroimidazo[1,2-a] benzimidazole derivatives against Leishmania donovani and Trypanosoma cruzi, Eur. J. Med. Chem. 84 (2014) 395–403, https://doi.org/10.1016/j.ejmech.2014.07.038.
[32] M. Alp, H. Göker, R. Brun, S. Yildiz, Synthesis and antiparasitic and antifungal evaluation of 2′-arylsubstituted-1H,1′H-[2,5′]bisbenzimidazolyl-5-carboxamidines, Eur. J. Med. Chem. 44 (2009) 2002–2008, https://doi.org/10.1016/j.ejmech.2008.10.003.
[33] J.M. Velázquez-López, A. Hernández-Campos, L. Yépez-Mulia, A. Téllez-Valencia, P. Flores-Carrillo, R. Nieto-Meneses, R. Castillo, Synthesis and trypanocidal activity of novel benzimidazole derivatives, Bioorg. Med. Chem. Lett 26 (2016) 4377–4381, https://doi.org/10.1016/j.bmcl.2015.08.018.
[34] C. Karaaslan, M. Kaiser, R. Brun, H. Göker, Synthesis and potent antiprotozoal activity of mono/di amidino 2-anilinobenzimidazoles versus Plasmodium falciparum and Trypanosoma brucei rhodesiense, Bioorg. Med. Chem. 24 (2016) 4038–4044, https://doi.org/10.1016/j.bmc.2016.06.047.
[35] S.A. Bakunov, S.M. Bakunova, T. Wenzler, M. Ghebru, K.A. Werbovetz, R. Brun, R.R. Tidwell, Synthesis and antiprotozoal activity of cationic 1,4-diphenyl-1H-1,2,3- triazoles, J. Med. Chem. 53 (2010) 254–272, https://doi.org/10.1021/jm901178d.
[36] P. Nagendar, J.R. Gillespie, Z.M. Herbst, R.M. Ranade, N.M.R. Molasky, O. Faghih, R.M. Turner, M.H. Gelb, F.S. Buckner, Triazolopyrimidines and imidazopyridines: structure-activity relationships and in vivo efficacy for trypanosomiasis, ACS Med. Chem. Lett. 10 (2019) 105–110, https://doi.org/10.1021/acsmedchemlett.8b00498.
[37] M. Hranjec, K. Starčević, B. Zamola, S. Mutak, M. Derek, G. Karminski-Zamola, New amidino-benzimidazolyl derivatives of tylosin and desmycosin, J. Antibiot. (Tokyo) 55 (2002) 308–314, https://doi.org/10.7164/antibiotics.55.308.
[38] S.R. Wilkinson, M.C. Taylor, D. Horn, J.M. Kelly, I. Cheeseman, A mechanism for cross-resistance to nifurtimox and benznidazole in trypanosomes, Proc. Natl. Acad. Sci. U. S. A 105 (2008) 5022–5027, https://doi.org/10.1073/pnas.0711014105.
[39] P. O'Sullivan, I. Rozas, Understanding the guanidine-like cationic moiety for optimal binding into the DNA minor groove, ChemMedChem 9 (2014) 2065–2073, https://doi.org/10.1002/cmdc.201402264.
[40] C.H. Ríos Martínez, L. Lagartera, C. Trujillo, C. Dardonville, Bisimidazoline arylamides binding to the DNA minor groove: N1-hydroxylation enhances binding affinity and selectivity to AATT sites, Medchemcomm 6 (2015) 2036–2042, https://doi.org/10.1039/c5md00292c.
[41] J. Parish, Principles of Nucleic Acid Structure: by W Saenger, Springer-Verlag, New York, 1984, p. 556, https://doi.org/10.1016/0307-4412(85)90046-9. DM 79. ISBN 3-540-90761-0, Biochem. Educ. 13 (1985) 92-92.
[42] P.R.S.C.R. Cantor, Biophysical Chemistry, W.H. Freeman and Co., San Francisco, 1980.
[43] G. Scatchard, The attractions of proteins for small molecules and ions, Ann. N. Y. Acad. Sci. 51 (1949) 660–672, https://doi.org/10.1111/j.1749-6632.1949.tb27297.x.
[44] J.L. Mergny, L. Lacroix, Analysis of thermal melting curves, Oligonucleotides 13 (2003) 515–537, https://doi.org/10.1089/154545703322860825.
[45] M. Radić Stojković, S. Miljanić, K. Mišković, L. Glavaš-Obrovac, I. Piantanida, The phenanthridine biguanides efficiently differentiate between dGdC, dAdT and rArU sequences by two independent, sensitive spectroscopic methods, Mol. Biosyst. 7 (2011) 1753–1765, https://doi.org/10.1039/c1mb05030c.
[46] Alison Rodger, Bengt Nordén, Circular Dichroism and Linear Dichroism, Oxford University Press, New York, 1997.
[47] R.W.W. Nina Berova, Koji Nakanishi (Eds.), Circular Dichroism: Principles and Applications, second ed., Wiley-VCH, New York, 2000 second ed.
[48] M. Eriksson, B. Nordén, Linear and circular dichroism of drug-nucleic acid complexes, Methods Enzymol. 340 (2001) 68–98, https://doi.org/10.1016/S0076-6879(01)40418-6.
[49] T. Šmidlehner, I. Piantanida, G. Pescitelli, Polarization spectroscopy methods in the determination of interactions of small molecules with nucleic acids - Tutorial, Beilstein J. Org. Chem. 14 (2017) 84–105, https://doi.org/10.3762/bjoc.14.5.
[50] M. Radić Stojković, I. Piantanida, Tuning urea-phenanthridinium conjugates for DNA/RNA and base pair recognition, Tetrahedron 64 (2008) 7807–7814, https://doi.org/10.1016/j.tet.2008.05.142.
[51] H.M. Berman, J. Westbrook, Z. Feng, G. Gilliland, T.N. Bhat, H. Weissig, I.N. Shindyalov, The protein data bank, Nucleic Acids Res. 28 (2000) 235–242, https://doi.org/10.1093/nar/28.1.235. www.rcsb.org.
[52] S.K. Burley, H.M. Berman, C. Bhikadiya, C. Bi, L. Chen, L. Di Costanzo, C. Christie, K. Dalenberg, J.M. Duarte, S. Dutta, Z. Feng, S. Ghosh, D.S. Goodsell, R.K. Green, V. Guranović, D. Guzenko, B.P. Hudson, T. Kalro, Y. Liang, R. Lowe, H. Namkoong, E. Peisach, I. Periskova, A. Prlić, C. Randle, A. Rose, P. Rose, R. Sala, M. Sekharan, C. Shao, L. Tan, Y.P. Tao, Y. Valasatava, M. Voigt, J. Westbrook, J. Woo, H. Yang, J. Young, M. Zhuravleva, C. Zardecki, RCSB Protein Data Bank: biological macromolecular structures enabling research and education in fundamental biology, biomedicine, biotechnology and energy, Nucleic Acids Res. 47 (2019) D464–D474, https://doi.org/10.1093/nar/gky1004.
[53] M.L. Barcellona, E. Gratton, Fluorescence lifetime distributions of DNA-4′,6-diamidino-2-phenylindole complex, BBA - Gen. Subj. 993 (1989) 174–178, https://doi.org/10.1016/0304-4165(89)90160-8.
[54] B. Nguyen, M.P.H. Lee, D. Hamelberg, A. Joubert, C. Bailly, R. Brun, S. Neidle, W.D. Wilson, Strong binding in the DNA minor groove by an aromatic

diamidine with a shape that does not match the curvature of the groove, J. Am. Chem. Soc. 124 (2002) 13680–13681, https://doi.org/10.1021/ja027953c.
[55] Y. Miao, M.P.H. Lee, G.N. Parkinson, A. Batista-Parra, M.A. Ismail, S. Neidle, D.W. Boykin, W.D. Wilson, Out-of-shape DNA minor groove binders: induced fit interactions of heterocyclic dications with the DNA minor groove, Biochemistry 44 (2005) 14701–14708, https://doi.org/10.1021/bi051791q.
[56] S. Mukherjee, S. Kundu, D. Bhattacharyya, Temperature effect on poly(-dA).poly(dT): molecular dynamics simulation studies of polymeric and oligomeric constructs, J. Comput. Aided Mol. Des. 28 (2014) 735–749, https://doi.org/10.1007/s10822-014-9755-x.
[57] M. Lõkov, S. Tshepelevitsh, A. Heering, P.G. Plieger, R. Vianello, I. Leito, On the basicity of conjugated nitrogen heterocycles in different media, Eur. J. Org Chem. 2019 (2017) 4475–4489, https://doi.org/10.1002/ejoc.201700749.
[58] E.D. Raczyńska, General structure–basicity relations for trisubstituted acetamidines, J. Chem. Soc. Perkin Trans. 2 (1987), https://doi.org/10.1039/P29870001117, 1117–1110.
[59] H.K. Hall, R.B. Bates, Correlation of alkylamine nucleophilicities with their basicities, Tetrahedron Lett. 53 (2012) 1830–1832, https://doi.org/10.1016/j.tetlet.2012.01.128.
[60] C. Fleau, A. Padilla, J. Miguel-Siles, M.T. Quesada-Campos, I. Saiz-Nicolas, I. Cotillo, J. Cantizani Perez, R.L. Tarleton, M. Marco, G. Courtemanche, Chagas disease drug discovery: multiparametric lead optimization against trypanosoma cruzi in acylaminobenzothiazole series, J. Med. Chem. 62 (2019) 10362–10375, https://doi.org/10.1021/acs.jmedchem.9b01429.
[61] N.T. Chandrika, S.K. Shrestha, H.X. Ngo, S. Garneau-Tsodikova, Synthesis and investigation of novel benzimidazole derivatives as antifungal agents, Bioorg. Med. Chem. 24 (2016) 3680–3686, https://doi.org/10.1016/j.bmc.2016.06.010.
[62] P.A. Greenidge, C. Kramer, J.C. Mozziconacci, R.M. Wolf, MM/GBSA binding energy prediction on the PDBbind data set: successes, failures, and directions for further improvement, J. Chem. Inf. Model. 53 (2013) 201–209, https://doi.org/10.1021/ci300425v.
[63] C. Xiao, Y. Cheng, Y. Zhang, J. Ding, C. He, X. Zhuang, X. Chen, Side chain impacts on pH- and thermo-responsiveness of tertiary amine functionalized polypeptides, J. Polym. Sci. Part A Polym. Chem. 52 (2014) 671–679, https://doi.org/10.1002/pola.27048.
[64] R. Kumar, J. Arora, A.K. Prasad, N. Islam, A.K. Verma, Synthesis and antimicrobial activity of pyrimidine chalcones, Med. Chem. Res. 22 (2013), https://doi.org/10.1007/s00044-013-0555-y, 56624–5631.
[65] T.S. Rodrigues, A.G.M. da Silva, L.C. de Oliveira, A.M. da Silva, R.R. Teixeira, P.H.C. Camargo, Cu2O spheres as an efficient source of catalytic Cu(I) species for performing azide-alkyne click reactions, Tetrahedron Lett. 58 (2017) 590–595, https://doi.org/10.1016/j.tetlet.2017.01.005.
[66] T.T.T. Maulik R. Patel, Aaditya Bhatt, Jamin D. Steffen, Adel Chergui, Junko Murai, Yves Pommier, John M. Pascal, Louis D. Trombetta, Frank R. Fronczek, Discovery and structure-activity relationship of novel 2,3-dihydrobenzofuran-7-carboxamide and 2,3-dihydrobenzofuran-3(2H)-one-7-carboxamide derivatives as poly(ADP-ribose)polymerase-1 inhibitors, J. Med. Chem. 57 (2014) 5579–5601, https://doi.org/10.1021/jm5002502.
[67] K.R. Senwar, T.S. Reddy, D. Thummuri, P. Sharma, V.G.M. Naidu, G. Srinivasulu, N. Shankaraiah, Design, synthesis and apoptosis inducing effect of novel (Z)-3-(3′-methoxy-4′-(2-amino-2-oxoethoxy)-benzylidene)indolin-2-ones as potential antitumour agents, Eur. J. Med. Chem. 118 (2016) 34–46, https://doi.org/10.1016/j.ejmech.2016.04.025.
[68] T.Y. Zhang, Z.K. Yu, X.J. Jin, M.Y. Li, L.P. Sun, C.J. Zheng, H.R. Piao, Synthesis and evaluation of the antibacterial activities of aryl substituted dihydrotriazine derivatives, Bioorg. Med. Chem. Lett 28 (2018) 1657–1662, https://doi.org/10.1016/j.bmcl.2018.03.037.
[69] X. Bu, H. Jing, L. Wang, T. Chang, L. Jin, Y. Liang, Organic base catalyzed O-alkylation of phenols under solvent-free condition, J. Mol. Catal. Chem. 259 (2006) 121–124, https://doi.org/10.1016/j.molcata.2006.06.009.
[70] N.W. Keigo Tanaka, Eiichi Yamamoto, Pyridine Derivative Substituted with Heterocycle and Phosphonoamino and Antifungal Agent Containing the Same, 2008. WO2008136324A1.
[71] I.N. Nnamani, G.S. Joshi, R. Danso-Danquah, O. Abdulmatik, T. Asakuru, D.J. Abraham, M.K. Safo, Pyridyl derivatives of benzaldehyde as potential antisickling agents, Chem. Biodivers. 5 (2008) 1762–1769, https://doi.org/10.1002/cbdv.200890165.
[72] Y. Pourshojaei, A. Gouranourimi, S. Hekmat, A. Asadipour, S. Rahmani-Nezhad, A. Moradi, H. Nadri, F.H. Moghadam, S. Emami, A. Foroumadi, A. Shafiee, Design, synthesis and anticholinesterase activity of novel benzylidenechroman-4-ones bearing cyclic amine side chain, Eur. J. Med. Chem. 97 (2015) 181–189, https://doi.org/10.1016/j.ejmech.2015.04.055.
[73] A.S. Judd, A.J. Souers, D. Wodka, G. Zhao, M.M. Mulhern, R.R. Iyengar, J. Gao, J.K. Lynch, J.C. Freeman, H.D. Falls, S. Brodjian, B.D. Dayton, R.M. Reilly, G. Gintant, J.T. Limberis, A. Mikhail, S.T. Leitza, K.A. Houseman, G. Diaz, E.N. Bush, R. Shapiro, V. Knourek-Segel, L.E. Hernandez, K.C. Marsh, H.L. Sham, C.A. Collins, P.R. Kym, Identification of diamino chromone-2-carboxamides as MCHr1 antagonists with minimal hERG channel activity, Bioorg. Med. Chem. Lett 17 (2007) 2365–2371, https://doi.org/10.1016/j.bmcl.2006.11.068.
[74] R. Bansal, G. Kumar, S. Rohilla, K.N. Klotz, S. Kachler, L.C. Young, A.L. Harvey, Synthesis and evaluation of a new series of 8-(2-Nitroaryl)Xanthines as adenosine receptor ligands, Drug Dev. Res. 77 (2016) 241–250, https://doi.org/10.1002/ddr.21317.
[75] Y. Yadav, E.D. MacLean, A. Bhattacharyya, V.S. Parmar, J. Balzarini, C.J. Barden, C.K.L. Too, A. Jha, Design, synthesis and bioevaluation of novel candidate selective estrogen receptor modulators, Eur. J. Med. Chem. 46 (2011) 3858–3866, https://doi.org/10.1016/j.ejmech.2011.05.054.
[76] R. Bansal, G. Kumar, D. Gandhi, L.C. Young, A.L. Harvey, Synthesis of a series of 8-(substituted-phenyl)xanthines and a study on the effects of substitution pattern of phenyl substituents on affinity for adenosine A1 and A2A receptors, Eur. J. Med. Chem. 44 (2009) 2122–2127, https://doi.org/10.1016/j.ejmech.2008.10.017.
[77] M.C. Taylor, M.D. Lewis, A.F. Francisco, S.R. Wilkinson, J.M. Kelly, The trypanosoma cruzi vitamin C dependent peroxidase confers protection against oxidative stress but is not a determinant of virulence, PLoS Neglected Trop. Dis. 9 (2015), e000370, https://doi.org/10.1371/journal.pntd.0003707.
[78] J.B. Chaires, N. Dattagupta, D.M. Crothers, Studies on interaction of anthracycline antibiotics and deoxyribonucleic acid: equilibrium binding studies on interaction of daunomycin with deoxyribonucleic acid, Biochemistry 21 (1982) 3933–3940, https://doi.org/10.1021/bi00260a005.
[79] J.L. Bresloff, D.M. Crothers, Equilibrium studies of ethidium-polynucleotide interactions, Biochemistry 20 (1981) 3547–3553, https://doi.org/10.1021/bi00515a038.
[80] T.V. Chalikian, J. Völker, G.E. Plum, K.J. Breslauer, A more unified picture for the thermodynamics of nucleic acid duplex melting: a characterization by calorimetric and volumetric techniques, Proc. Natl. Acad. Sci. U. S. A 96 (1999) 7853–7858, https://doi.org/10.1073/pnas.96.14.7853.
[81] R.A. Friesner, R.B. Murphy, M.P. Repasky, L.L. Frye, J.R. Greenwood, T.A. Halgren, P.C. Sanschagrin, D.T. Mainz, Extra precision glide: docking and scoring incorporating a model of hydrophobic enclosure for protein-ligand complexes, J. Med. Chem. 49 (2006) 6177–6196, https://doi.org/10.1021/jm051256o.
[82] T.A. Halgren, R.B. Murphy, R.A. Friesner, H.S. Beard, L.L. Frye, W.T. Pollard, J.L. Banks, Glide: a new approach for rapid, accurate docking and scoring. 2. Enrichment factors in database screening, J. Med. Chem. 47 (2004) 1750–1759, https://doi.org/10.1021/jm030644s.
[83] R.A. Friesner, J.L. Banks, R.B. Murphy, T.A. Halgren, J.J. Klicic, D.T. Mainz, M.P. Repasky, E.H. Knoll, M. Shelley, J.K. Perry, D.E. Shaw, P. Francis, P.S. Shenkin, Glide: a new approach for rapid, accurate docking and scoring. 1. Method and assessment of docking accuracy, J. Med. Chem. 47 (2004) 1739–1749, https://doi.org/10.1021/jm0306430.
[84] Schrödinger Release 2019-3: Glide, Schrödinger, LLC, New York, NY, 2019.
[85] Schrödinger Release 2019-3, Schrödinger, LLC, New York, NY, 2017.
[86] J. Li, R. Abel, K. Zhu, Y. Cao, S. Zhao, R.A. Friesner, The VSGB 2.0 model: a next generation energy model for high resolution protein structure modeling, Proteins Struct. Funct. Bioinforma. 79 (2011) 2794–2812, https://doi.org/10.1002/prot.23106.
[87] W.L. Jorgensen, D.S. Maxwell, J. Tirado-Rives, Development and testing of the OPLS all-atom force field on conformational energetics and properties of organic liquids, J. Am. Chem. Soc. 118 (1996) 11225–11236, https://doi.org/10.1021/ja9621760.
[88] D. Shivakumar, J. Williams, Y. Wu, W. Damm, J. Shelley, W. Sherman, Prediction of absolute solvation free energies using molecular dynamics free energy perturbation and the opls force field, J. Chem. Theor. Comput. 6 (2010) 1509–1519, https://doi.org/10.1021/ct900587b.
[89] K.J. Bowers, E. Chow, H. Xu, R.O. Dror, M.P. Eastwood, B.A. Gregersen, J.L. Klepeis, I. Kolossvary, M.A. Moraes, F.D. Sacerdoti, J.K. Salmon, Y. Shan, D.E. Shaw, Scalable algorithms for molecular dynamics simulations on commodity clusters, in: Proc, ACM/IEEE Conf. Supercomput. SC'06, 2006, https://doi.org/10.1145/1188455.1188544, 2006.
[90] Schrödinger Release 2019-3: Desmond Molecular Dynamics System, D. E. Shaw Research, New York, NY, 2019.
[91] Maestro-Desmond Interoperability Tools, Schrödinger, New York, NY, 2019.
[92] ACD/Percepta, Version 2017.2.1, Advanced Chemistry Development, Inc., Toronto, On, Canada, 2019. www.acdlabs.com.
[93] P. Acharya, M.P. O'Connor, J.W. Polli, A. Ayrton, H. Ellens, J. Bentz, Kinetic identification of membrane transporters that assist P-glycoprotein-mediated transport of digoxin and loperamide through a confluent monolayer of MDCKII-hMDR1 cells, Drug Metab. Dispos. 36 (2008) 452–460, https://doi.org/10.1124/dmd.107.017301.